Aerospace Science and Technology 117 (2021) 106952

Contents lists available at ScienceDirect

Aerospace Science and Technology

www.elsevier.com/locate/aescte

Review

Advances in plasma-assisted ignition and combustion for combustors of aerospace engines

Mengzhe Li [a], Zhikai Wang [b], Rongguang Xu [c], Xiaoliang Zhang [c], Zhitong Chen [c,d,*], Qiu Wang [e,*]

[a] Science and Technology on Combustion, Internal Flow and Thermo-Structure Laboratory, Northwestern Polytechnical University, Xi'an 710072, China
[b] AECC Hunan Aviation Powerplant Research Institute, Zhuzhou 412002, China
[c] Department of Mechanical and Aerospace Engineering, The George Washington University, Washington, DC 20052, USA
[d] National Innovation Center for Advanced Medical Devices, Shenzhen 518000, China
[e] State Key Laboratory of High Temperature Gas Dynamics, Institute of Mechanics, Chinese Academy of Sciences, Beijing 100190, China

ARTICLE INFO

Article history:
Received 9 October 2020
Received in revised form 16 May 2021
Accepted 3 July 2021
Available online 13 July 2021
Communicated by Bing Wang

Keywords:
Non-equilibrium plasma
Plasma-assisted ignition
Plasma-assisted combustion
Aerospace engine
Combustor
Extreme condition

ABSTRACT

The improvement of the ignition and combustion performance of aerospace engines under extreme conditions such as high altitude, low temperature, low pressure, and high speed is a research topic of broad and current interest. Plasma technology has attracted increasing attention due to its significant potential in improving ignition and combustion performance. Scientists and engineers have conducted numerous investigations and experiments on the use of plasma technology in aerospace engines, especially in aviation gas turbine engines, driving the research and applications of plasma-assisted ignition (PAI) and plasma-assisted combustion (PAC). The aim of this comprehensive review paper is to summarize and discuss the developments and applications of PAI and PAC in the fields of aerospace engines during the last ten years, including ignition, lean blow-out, combustion efficiency, emission, outlet temperature distribution quality, combustion stability, and fuel distribution. This review paper mainly focuses on experimental research progress. We also introduce new applications of PAI and PAC in novel aerospace engines and discuss the prospects for its practical implementation.

1. Introduction

A combustor with a high-temperature rise and high stability can greatly increase the thrust-to-weight ratio or power-to-weight ratio for military aerospace engines [1]. As flight altitude increases and the speed and stability of combustion decrease, the engine combustor requires a relatively wide lean blow-out (LBO) boundary and high-temperature rise under extreme conditions. It also requires a temperature field with high quality at the exit of the combustor [2]. Due to economic and environmental considerations, reductions in fuel consumption and pollutant emissions are major goals in the development of combustors for civil aviation engines [3]. Therefore, high combustion efficiency and low pollutant emissions are required. Currently, several issues of the combustor, including high-altitude LBO/ignition and ignition envelopes smaller than the flight envelope, severely limit performance improvements of aerospace engines [4]. Plasma technology provides an effective method to improve ignition and combustion performance [5–7]. Plasma is generated by the gas discharge and the mixed gases are easily ignited due to the temperature rise effect, chemical reactions, and aerodynamic effect [8,9]. PAC refers to the collision processes between plasma-generated high-energy ions/electrons and fuel molecules. The breakage of the high-carbon chains of molecules into low-carbon chains stimulates active particles and generates a large number of reactions, which greatly improve the combustion reaction rate and combustion efficiency [1,10].

PAI and PAC in aerospace engines have been investigated for an extended period. Since the 1980s, UK Rolls-Royce Holdings PLC, UK, General Electric Company, US, Alpha Pro Tech Ltd., US, Princeton University, US, and the Russian Institute of High Temperature Physics Research have made important contributions to apply plasma technology to the ignition, combustion, and fuel atomization of the combustor [7]. At present, research on the PAI and PAC is mainly focused on non-equilibrium plasma [8]. The high-energy ions/electrons generated in non-equilibrium plasma collide with atoms, molecules, and other particles in combustible mix gas, producing a large number of oxygen atoms, ozone, and active particles

* Corresponding authors.
E-mail addresses: zt.chen@nmed.org.cn (Z. Chen), wangqiu@imech.ac.cn (Q. Wang).

https://doi.org/10.1016/j.ast.2021.106952

Nomenclature

ACDH	assisted combustion from dilution holes
ACPH	assisted combustion from primary holes
AI	artificial intelligence
ANN	artificial neural network
CC	conventional combustion
CRZ	central recirculation zone
CSI	conventional spark igniter
CZ	central zone
DBD	dielectric barrier discharge
ECN	engine combustion network
EINO*x*	emission index NO_x
FGM	flamelet generated manifolds
GA	genetic algorithms GAPFI gliding arc plasma fuel injector
ICAO	International Civil Aviation Organization
LBO	lean blow-out
LDI	lean direct injection
LPM	standard liters per minute
LPP	lean premixed prevaporized
LTO	landing and take-off
NLP	natural language processing
NO*x*	oxides of nitrogen
NSPD	nano-second pulsed plasma discharge
ORZ	outside recirculation zone
OTDF	overall temperature distribution factor
PAC	plasma-assisted combustion
PACA	plasma-assisted combustion actuator
PAI	plasma-assisted ignition
RQL	rich-quench-lean
RMPI	recessed multichannel plasma igniter
RMS	root mean square
RR	repetition rate
SN	swirl number
TAPS	twin annular premixing swirler
TPI	transient plasma ignition
TRL	technology readiness level
TVC	trapped-vortex combustor
U	applied voltage of plasma-assisted combustion actuator
α	the excess air coefficient
φ	fuel-to-air equivalence ratio

to initiate the chain oxidation reactions [9]. In addition, the ion wind generated in non-equilibrium plasma promotes the mixing of the fuel and increases the contact area between active particles and other particles, stimulating chain oxidation reactions and accelerating the combustion reaction process [10]. There are two methods of PAI and PAC: 1) the plasma is generated outside of the combustor and then introduced into the combustor, and 2) the plasma generator is located in the combustor to assist ignition and combustion [11]. PAI and PAC can increase the performance of the aerospace engine combustor, widen the range of combustion stability, improve the temperature distribution unevenness at the combustor exit, enhance the fuel combustion efficiency, and reduce pollutant emissions [12].

This comprehensive review focuses on PAI and PAC for combustors in aerospace engines, including ignition, LBO, combustion efficiency, emission, overall temperature distribution factor (OTDF), combustion stability, and fuel distribution. We discuss a broad range of PAI and PAC applications in new types of aerospace engines, as well as future developments and challenges. Although numerical simulations have made contributions in the study of PAI and PAC, detailed research is still limited, and numerical simulations urgently need to be verified by experimental results. Therefore, this review paper focuses on experimental progress.

2. Basic concepts and principles

2.1. Plasma

Plasma, partially or completely ionized gas, contains charged ions, free radicals, electrons, various active groups, and so on [13]. It is the fourth fundamental state of matter and is essentially different from the rest three states of matter: solid, liquid, and gas. Plasma can be divided into thermodynamic equilibrium and non-equilibrium plasma. In thermodynamic equilibrium plasma, electron, ion, and gas temperatures are completely consistent, while the electron temperature of the non-equilibrium plasma is much higher than ion and gas temperatures. The topics of degenerated quantum plasma and relativistic plasma are beyond the scope of plasma dynamics for aerospace engineering. Therefore, present discussions are focused on plasma that exists around atmospheric pressure, and on mixed thermal and non-thermal conditions. Description of plasma is usually by its energy state and degree of ionization. The classification of plasma is commonly recognized by the electron number density and temperature in electron volts or the static temperature as displaced in Fig. 1. It shows that non-equilibrium plasmas are characterized by weaker electron and ion densities in comparison to neutral molecules density. They are further characterized by a low ionization degree in contrast with thermal plasmas. It is worth noting that in such conditions, electron-neutral and ion-neutral collisions play important roles (excitation, ionization, dissociation) [11]. Generally, the plasma of interest for aerospace applications is limited to an electron number density up to 10^{20} /cm^3 and an overall temperature lower than 10^6 K.

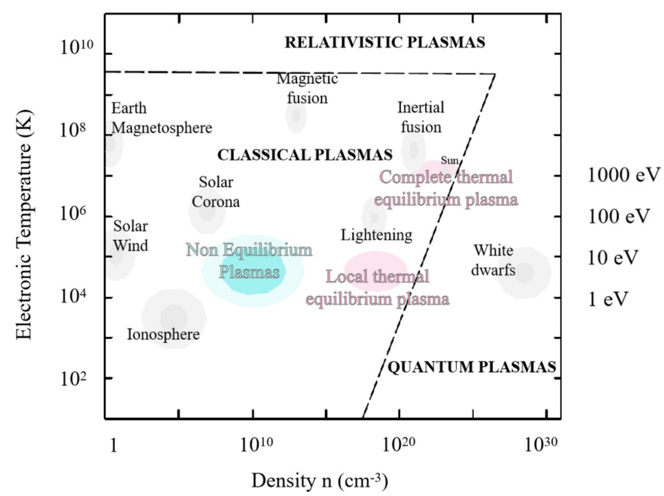

Fig. 1. Density-temperature diagram. Reproduced from [11].

Due to the high temperature of the thermodynamic equilibrium plasma, it generally can be used for combustion, cutting, welding, and other processes [14]. A typical application in combustion is the spark plug-assisted ignition [15]. The discharge of the spark plug generates thermodynamic equilibrium plasma, which induces local combustible gas molecules to be heated and ignited. However, this method with self-producing active substances depends on the concentration of reactants: it is hard to maintain combustion under rare and extreme conditions, such as at high altitudes and plateaus. In addition, most of the ignition energy is utilized to heat the electrodes and working gas, resulting in lower ignition efficiency. Here, non-equilibrium plasma has much stronger kinetic activity because electrons with higher temperature collide and induce decomposition and excitation subsequently rapidly forming a large number of active radicals, clusters, and excited particles. The uneven temperature fields of non-equilibrium plasma are beneficial to the progress of chemical reactions: high-energy electrons quickly activate the reactant molecules and gas temperature close to room temperature can ensure the activation of reactants without additional energy [12]. Plasma-assisted ignition, with the advantages of large ignition area, high energy, short delay time, and high success rate, broadens the ignition envelope and achieves rapid restart at high altitude. In addition, it improves the combustion efficiency and flame blow-out speed, which also expands the lean blow-out boundary and reduces pollutant emissions. Moreover, non-equilibrium plasma has a number of other applications, such as surface modification, material processing, microelectronics engineering, nanotechnology, energy, agriculture, environment, biomedicine, and so on [16–25].

2.2. Plasma-assisted ignition and combustion

PAI produces Joule heat by plasma discharge, which rapidly heats the working medium to form a high-temperature jet around 3000∼5000 K [26]. The temperature of the combustible mixture around the high temperature jet rises sharply to form a large area of activation and accelerate the ignition process. PAC uses the active particles generated in non-equilibrium plasma discharge to accelerate combustion particle reactions, thereby improving the fuel combustion performance [15]. Due to different mechanisms, a plasma igniter and a PAC exciter are two different combustor devices, resulting in different structures and external shapes for the combustors. Fig. 2 shows the schematic of the ignition and combustion in an aero-engine combustor with conventional spark combustion mode and PAI&PAC.

High energy electrons in plasma collide with atoms or molecules that are excited, dissociated, and ionized to generate a large number of active reaction components [26,28]. Moreover, plasma excitation will also produce intermediate species not generated in the conventional combustion system, causing a new reaction chain to change the combustion characteristic kinetics. Plasma discharge not only generates active components and heats the combustible mixture but disturbs the flow field and changes the combustion state of the gas mixture. There are three main mechanisms of PAI and PAC: thermal effects, chemical effects (chemical dynamics), and transport effects (aerodynamics) [29–31]. The thermal effects refer to the ability to instantly heat the medium in the discharge area and cause its temperature to rapidly rise (also called the temperature rise effect). The chemical effect is related to electrons colliding with air or fuel molecules, subsequently leading to the macromolecular hydrocarbon fuel being ionized into charged active particles with low energy, and finally to O_2 and N_2 in air being ionized into charged active particles which can oxidize active particles, thereby accelerating the chemical chain reaction [32]. The transport effects occur through flow field disturbance during the plasma discharge process as follows: 1) enhance the airflow turbulence in the combustor and increase the mixing of fuels and air as well as the contact area between the flame and the fresh mixture; 2) increase the directional migration of plasma in the mixed gas to expand the flame surface/front area and increase the propagation speed of flame, to enhance the stability of combustion [27,33,34]. Fig. 3 shows the schematic of the major enhancement pathways of plasma-assisted combustion, it indicates that plasma excitation generates heat, radicals, excited species, electrons/ions to induce fuel cracking and particle transport, and their synergetic effect further increases the fuel combustion efficiency.

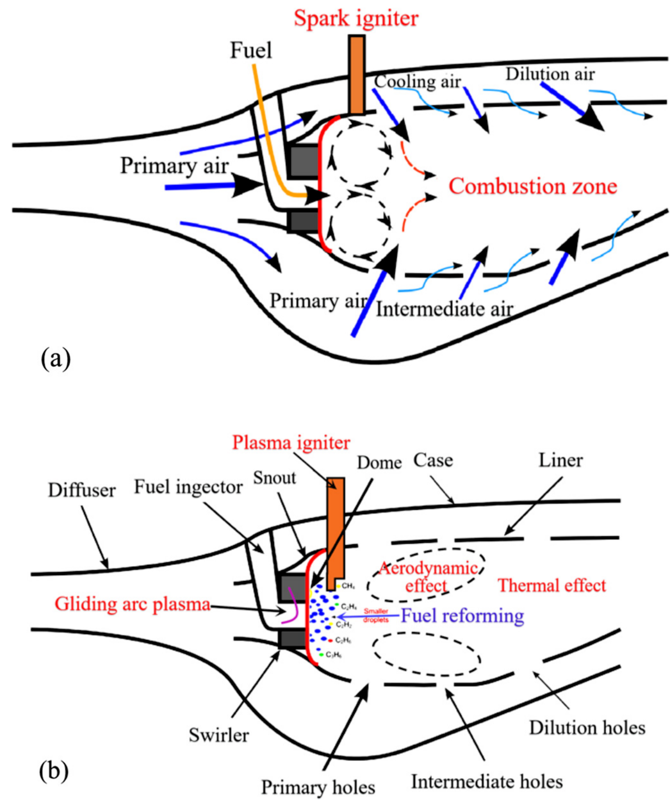

Fig. 2. The schematic of the ignition and combustion in aero-engine combustor: (a) Conventional spark combustion mode, (b) Plasma assisted ignition and combustion through plasma igniter or setting up gliding arc plasma at the combustor head.

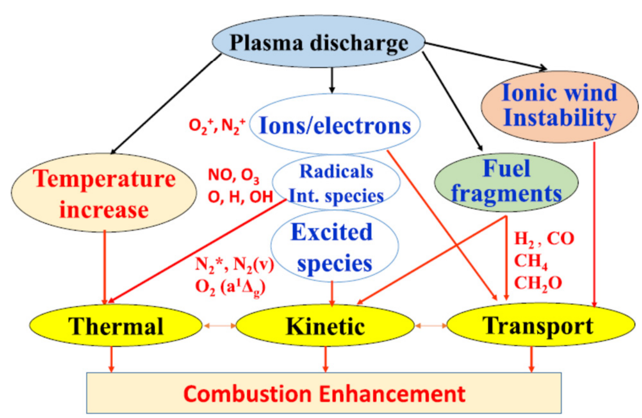

Fig. 3. The schematic of the major enhancement pathways of plasma-assisted combustion. Reproduced from [27].

3. Research progress of plasma in the combustor of aerospace engine

3.1. Performances for aero-engine combustor

The combustor is an important component of an aerospace gas turbine engine [35]. Its function is to release the chemical energy in the fuel through combustion with air entering the engine and

Table 1
An overview of 10-year progress on PAI and PAC in aero-engine/gas turbine combustor.

Research contents	Fuel	Investigation method	Combustor type	Year	Refs.
• Temperature • Vorticity • O_3	Methane/Air	Numerical simulation	Coaxial jet combustor	2020	[37]
• Ignition delay time • Spontaneous emission	Kerosene/Air	Experimental investigation	Model combustor	2020	[38]
• Ignition process • Flame shape • LBO • CH^*	Kerosene/Air	Experimental investigation	Swirl combustor	2020	[39]
• Discharge distribution • Lift-off height • LBO • OH^*	Methane/Air	Experimental investigation	Additive-manufactured thruster combustor	2020	[40]
• Ignition and flame propagation process • Temperature • Chemical reaction rate	Methane/Air	Numerical simulation	100 KW low-calorie fuel combustor	2020	[41]
• LBO • CO/NO_x	Methane/Air	Experimental investigation	Swirl-stabilized combustor	2020	[42]
• Combustion oscillation	Methane/Air	Experimental and numerical simulation	Cylindrical combustor	2019	[43]
• LBO • Flame expansion characteristics • Burning velocity • Maxstein length	Methane/Air	Experimental investigation	Constant volume combustor	2019	[44]
• Temperature • Combustion efficiency • OTDF	Kerosene/Air	Experimental investigation	Fan-shaped aero-engine annular combustor	2019	[45]
• Discharge characteristic • Flame shapes • Ignition delay time	Kerosene/Air	Experimental investigation	Model combustor	2019	[46]
• Temperature • Combustion efficiency • CO	Kerosene/Air	Numerical simulation	Aero-engine annular combustor	2019	[47]
• Swirling flow and flame shape • pressure fluctuation spectra • Static flame stability and emission	Methane/Air	Experimental investigation	Realistic gas turbine combustor	2019	[48]
• Inlet air temperature • Outlet highest temperature • OTDF • Ignition boundary	Kerosene/Air	Experimental investigation	Aero-engine reverse-flow combustor	2019	[49]

transform it into thermal energy, leading to a rapid expansion of the gas due to the increase in total enthalpy. High-energy gas is able to do work in the turbine and the exhaust nozzle. From the perspective of engineering thermodynamics, the combustor is an energy conversion device. The combustor of an aviation gas turbine needs to work stably in a wide range of conditions, be started reliably, and allow the engine to be accelerated to the rated state in a short time [36]. Therefore, certain performance indicators must be met to satisfy the operating conditions of the engine. The performance indicators of the combustor are as follows: (1) combustion efficiency; (2) starting ignition and high-altitude re-ignition; (3) stable working range; (4) total pressure loss coefficient; (5) outlet temperature distribution; (6) exhaust air pollution; (7) durability; (8) combustion instability; (9) size and structure; (10) maintainability.

Due to the performance requirements of high-altitude ignition in aero-engines, the use of plasma in the combustor of aero-engines for ignition and combustion-supporting applications is attracting increasing attention. Researchers across the globe have carried out an extensive investigation of transport effects. Table 1 summarizes the research on PAI and combustion-supporting technology in the field of aero-engine and gas turbine combustors in the past ten years.

3.2. Ignition performance

The ignition performance of the combustor is the first important link in the reliable operation of an aerospace engine and should be investigated first. The key parameter for its evaluation is the fuel-air ratio of lean ignition. At present, common ignition methods of the combustor include electric spark ignition and plasma ignition.

Because of its small size, simple structure, and ease of use, the spark igniter is the most widely used form of ignition [86]. It can convert electrical energy into thermal energy in a relatively small volume, and it can also realize a complete control of the ignition frequency, and the duration of energy released by each discharge. A high-energy ignition device is shown in Fig. 4. The electric spark ignition system adopted is mainly composed of a driving power supply, ignition coil, ignition nozzle, ignition cable, etc. The boost

Table 1 (*continued*)

Research contents	Fuel	Investigation method	Combustor type	Year	Refs.
• Emissions • Combustion efficiency • Outlet temperature	Kerosene/Air	Experimental investigation	Aero-engine annular combustor	2019	[50]
• Temperature • Lean ignition limit • Discharge process • Chemical reaction rate	$C_{12}H_{23}$	Experimental and numerical investigations	Can-annular combustor of gas turbine	2019	[51]
• Discharge characteristics • Ignition limit • LBO • Fuel reforming/SMD • Sequential images of flame	Kerosene/Air	Experimental investigation	GAPFI swirl combustor	2019	[52]
• Temperature • Combustion efficiency • OTDF/RTDF • LBO	Kerosene/Air	Experimental investigation	Fan-shaped aero-engine annular combustor	2019	[53]
• Rate of heat release • Ignition delay time • Temperature • Damköhler number	CH_4/N_2	Numerical investigation	Three-coaxial burner	2019	[54]
• Plasma ignition voltage characteristics • Ignition process	$C_{12}H_{23}$	Experimental and numerical investigations	Can-annular combustor of gas turbine	2019	[55,56]
• OTDF • CO • temperature	Methane/Air	Numerical simulation	Semi-cylindrical bluff-body combustor	2018	[56]
• Electrical characteristics • Ignition process • Ignition delays times	Kerosene/Air	Experimental investigation	V-shaped burner	2018	[57]
• Turbulent premixed flame	Methane/Air	Experimental investigation	Dump burner	2018	[58]
• Discharge characteristic • Spectrum characteristic • Jet characteristic • Ignition characteristic	Kerosene/Air	Experimental investigation	Model combustor	2018	[59]
• Lean ignition limits • Ignition delay time • Crossfire generated	Kerosene/Air	Experimental investigation	Aero-engine reverse-flow combustor	2018	[60]
• LBO • Sequential images of flame • CO/NO_x • Combustion Dynamics	Fuel/Air	Experimental investigation	Lean Direct Injection (LDI) combustor	2017	[61]
• Combustion stability • NO_x/CO	Methane/Air	Experimental investigation	Model gas turbine combustor	2017	[62]
• Combustion efficiency • LBO	Kerosene/Air	Experimental investigation	Model combustor	2016	[63]
• Discharge characteristic • Jet characteristic • Process of kerosene/air mixture igniting	Kerosene/Air	Experimental investigation	Model combustor	2016	[64]
• Flammability limits and flame structure • Optical emission spectroscopy	Natural gas/Air	Experimental investigation	Vortex chamber	2016	[65]
• Flame dynamics and stability • LBO	Methane/Air	Experimental investigation	Swirl-stabilized combustor	2016	[66]
• LBO • Flame Stabilization • OH number density • Spectrally Resolved Emission	Methane/Air	Experimental investigation	Swirl-stabilized combustor	2016	[67]
• Flame stability • LBO	Propane/Air	Experimental investigation	Swirl combustor	2015	[68]

(*continued on next page*)

Table 1 (*continued*)

Research contents	Fuel	Investigation method	Combustor type	Year	Refs.
• Emissions • Combustion efficiency • Swirling flow and flame shape • Dynamic combustion instabilities	Methane/Air	Experimental investigation	Dump combustor	2015	[69]
• The effects of O_3	Methane/Air	Experimental and numerical investigations	Low swirl burner	2015	[70]
• Flame shape • LBO	Methane/Air	Experimental investigation	Microburner	2015	[71]
• Velocity • Temperature • Pressure • Turbulent kinetic energy	Kerosene/Air	Numerical investigation	Single cup combustor	2015	[72]
• Ignition delay time • Temperature • OH concentration	Hydrogen/Air	Experimental investigation	Plasma flow reactor	2014	[73]
• Ignition process • Temperature • Ignition delay time	Propane/Air	Experimental investigation	Model combustor	2013	[74]
• Combustion oscillations • Flame shape	–	Experimental investigation	Swirl-stabilized combustor	2013	[75]
• CH^* • OH LIF • Temperature • Flame position/lift-off height	Propane/Air	Experimental investigation	Bluff-body combustor	2013	[76]
• $NO/NO_2/CO$ • CH^*	Natural gas/Air	Experimental investigation	Swirl-stabilized combustor	2013	[77]
• NO_x/CO • Flame shape	Liquefied petroleum gas/Air	Experimental investigation	Staged combustor	2013	[78]
• Ignition process • Temperature • Ignition delay time	Propane/Air	Numerical investigation	Model combustor	2013	[79]
• Ignition delay time • Temperature • OH concentration	Hydrogen/Air	Experimental investigation	Plasma flow reactor	2013	[80,81]
• $NO_x/CO/THC$ • Flame shape	Liquefied petroleum gas/Air	Experimental investigation	Staged combustor	2012	[82]
• Combustion products (O_2/CO)	Propane/Air	Experimental investigation	Model combustor	2012	[83]
• Hydroxyl radical kinetics	Hydrogen/Air	Experimental investigation	Plasma flow reactor	2011	[84]
• Temperature • NO_x	–	Experimental and numerical investigation	25 MW gas turbine combustor	2011	[85]

rectification in the ignition coil is converted into a DC pulsating current, which charges the energy storage capacitor. When the capacitor is full, the discharge current is transmitted to the ignition tip through the discharge tube, choke coil, and ignition cable, forming a high-energy arc spark [87].

The process of electric spark ignition is as follows [87,88]. According to the principle of the combustor ignition and circumferential flame propagation, the ignition process consists of three stages: 1) initial fire core formation, 2) fire core expansion and development to form a single stable swirling flame, and 3) circumferential propagation of the flame and ignition of all nozzles. The three-stage schematic diagram of the spark ignition process is shown in Fig. 5, and the spark ignition test process is shown in Fig. 6.

PAI is a relatively new type of advanced ignition method, which has great application prospects in the aerospace field and under extreme conditions of ignition. Compared with the electric spark igniter, the plasma igniter has the advantages of large discharge energy, soot resistance, and especially when it is ignited, a strengthening effect on combustion. The PAI system uses air as the working medium, and it is mainly composed of a plasma igniter, a driving power supply, and a gas supply system [60]. The plasma igniter is a non-transferred arc plasma jet igniter with high frequency and high voltage pulse ignition. The cathode and anode are made of 75% tungsten copper alloy, which is resistant to high temperature and corrosion, and has good electrical conductivity. The working medium adopts lateral air intake. When the ignition gas (air) passes through the channel between the cathode and the anode, a high-temperature plasma arc is generated under the action of the plasma power source, and it is ejected in the form of a high-temperature jet.

The PAI process is as follows. The power supply is turned on, and the plasma igniter ignites the gas in the combustor: (1) the plasma generator discharge breaks down the air medium, produces a high temperature plasma jet rich in active particles, and forms an initial high-temperature fire core; (2) the formed initial fire nucleus ignites the mixed gas to form a secondary fire nucleus; (3) the flame front propagates to the central reflux area of the combustor, so that the combustor can be ignited, as shown in Fig. 7.

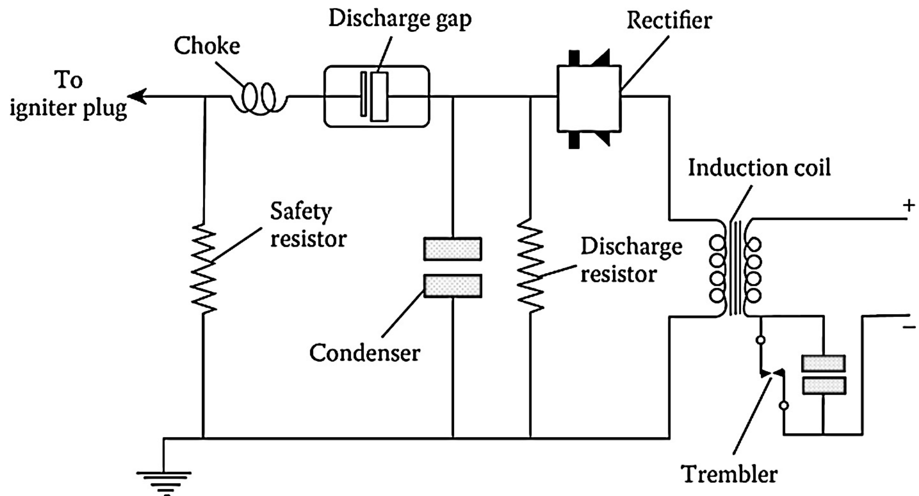

Fig. 4. Standard high-energy ignition unit. Reproduced from [87].

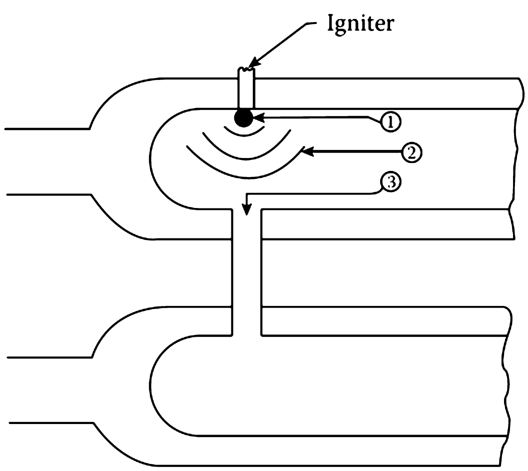

Fig. 5. Three-phase nature of the ignition process. Reproduced from [87].

Fig. 8 shows a comparison of the ignition process of a kerosene/air mixture using plasma jet ignition and electric spark ignition. The flame core area is much larger during PAI than electric spark ignition. The combustible mixture in the area around the PAI jet is rapidly ignited, and the flame propagates to the unburned area at a higher speed, significantly reducing the ignition delay.

Liu et al. studied the effect of increasing/not increasing the active components on the ignition boundary [51]. It can be seen from Fig. 9 that the increase of active plasma components can significantly broaden the lean ignition boundary of the combustor, indicating that the active particles play an important role in accelerating the chemical reaction and increasing the flame propagation speed. The main reason is that the active particles such as O, NO, and O_3 in the plasma can obviously promote the ignition of the fuel. In particular, the Air Force Engineering University of China proposed a type of recessed multichannel plasma igniter (RMPI) in three-channel and five-channel configurations [90]. Compared with the conventional spark igniter (CSI), the RMPI has a shorter ignition delay time and faster flame development, which can effectively broaden the lean ignition boundary. A three-channel plasma igniter can widen the lean ignition boundary by 18%, while a five-channel igniter can broaden the ignition boundary by 31%. Therefore, the RMPI is more capable of achieving fast and reliable ignition.

Zhao et al. studied the influence of spark ignition and PAI on ignition delay time, as shown in Fig. 10 [38]. The results show that a plasma jet ignition delay time is much shorter than that for spark ignition in a wide range of excess air coefficients; the minimum plasma jet ignition delay time shows a decrease of 88.74% when compared to spark ignition in the same experimental conditions. The main reason is that the active particles produced by plasma discharge can significantly increase the chemical reaction rate of the kerosene/air mixture: the active particles participate in the chemical reaction of combustion, accelerate the combustion reaction, and shorten the ignition delay time. Moreover, related studies have shown that the higher the concentration of active particles is, the shorter the resulting ignition delay time becomes [55]. The effect of the PAI and PAC becomes more evident with the increase in particle concentration [47]. Adding plasma to the combustor can reduce the critical ignition power and critical ignition duration time to a certain extent [41].

Compared with traditional electric spark ignition, PAI has the following advantages [91–94]. (1) Large ignition area: traditional electric spark ignition is usually a point-to-point ignition method, and the ignition area of PAI can be a surface or even a three-dimensional space. A large number of ignition streams can achieve simultaneous ignition at multiple points, significantly increasing the reliability of PAI. (2) The ignition delay time is short. PAI has greater ignition energy than electric spark ignition, which can quickly increase the temperature of the combustible mixture around the ignition area, make the combustible mixture quickly reach the combustion reaction conditions, and shorten the ignition delay time. (3) High utilization rate of ignition energy. In traditional spark ignition, only a small part of the electric energy is converted into ignition energy, and a large amount of electric energy is used for light emission and heating electrodes, in comparison, most of the electric energy consumed by PAI is used for ignition, thereby improving the utilization rate of ignition energy. (4) The combustible mixture is converted into activated particles for combustion reaction, which greatly reduces the generation of intermediate products, makes the combustion reaction more complete, improves the fuel utilization rate, and greatly reduces the emission of harmful substances. (5) The ignition energy can be better coupled with the combustible mixture. The macromolecular hydrocarbon fuel in the ignition area is ionized into active particles with small activation energy, which increases the chemical reaction rate of the combustible mixture and shortens the reaction time, thereby improving the ignition performance.

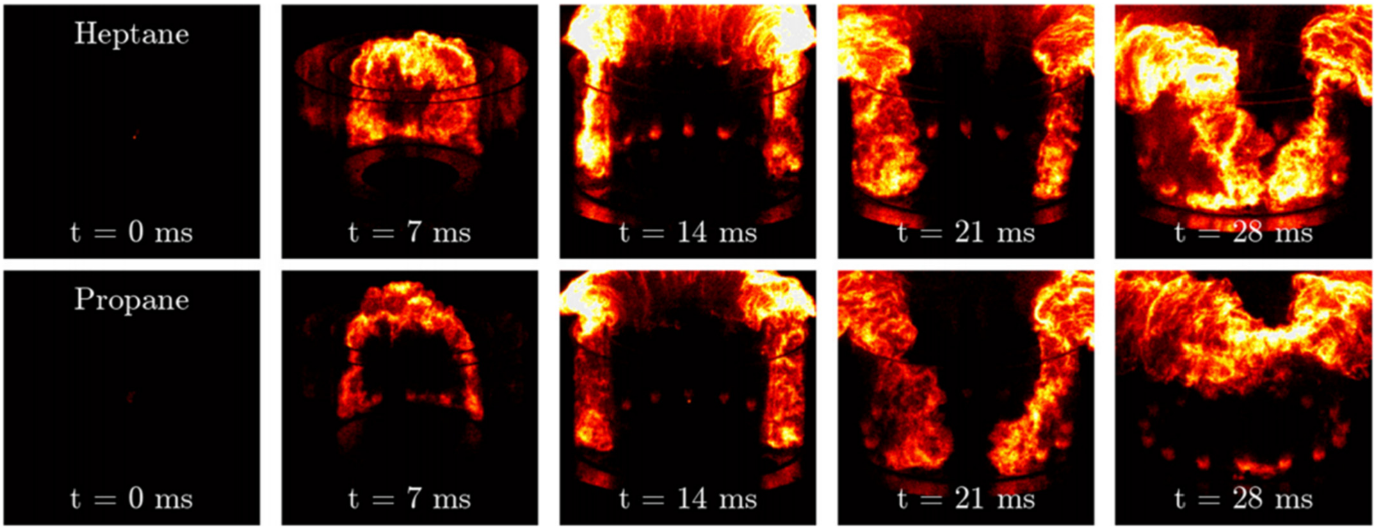

Fig. 6. Light emission during the ignition sequence of propane (top) and n-heptane (bottom) fuels. Yellow corresponds to high light intensity, and dark red represents low light emission. Reproduced from [89]. (For interpretation of the colors in the figure(s), the reader is referred to the web version of this article.)

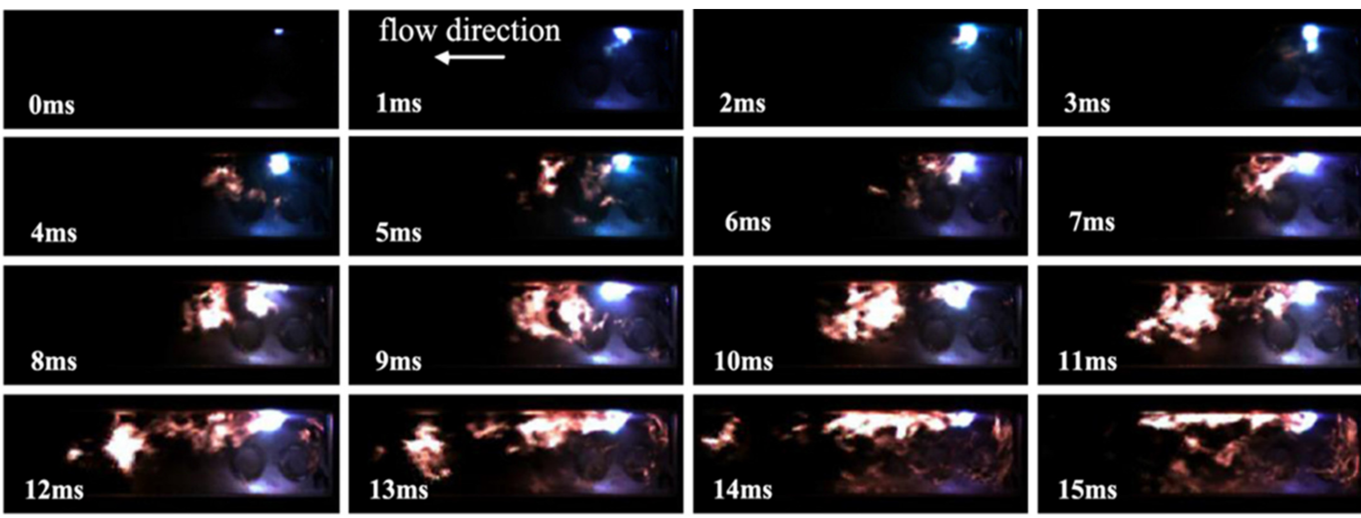

Fig. 7. The processes of plasma ignition with a DC plasma jet igniter. The output voltage of the designed plasma igniter is 100–170 V which depends on the gas flow rate, power output current, plasma gas composition, and nozzle design. Reproduced from [57].

3.3. Characteristics of lean blowout (LBO)

With the continuous increase in the thrust-to-mass ratio of aero-engines and the increase in the fuel-air ratio of the combustor, conventional combustors face greater challenges: increasing fuel supply to achieve a high fuel-air ratio will lead to an increase in the equivalent ratio of the main combustion zone, resulting in a large amount of smoke in the heavy-duty state; if the smoke is reduced by increasing the air intake of the main combustion zone, it will cause the poor performance of a lean blowout under the light-duty state of the combustor. Therefore, improving the fuel-air ratio while maintaining the LBO performance is an important issue [95]. Fig. 11 shows photos of flameout tests, where Fig. 11(a) is the test of the PAC ($\alpha = 1$), while Fig. 11(b) is the test of the lean blowout limit (the excess air coefficient near the flameout).

The enhancement of the gliding arc plasma fuel injector (GAPFI) is supposed to work via three pathways: thermal, kinetic, and transport effects. Sequential images of flame with plasma and without plasma at a decreasing equivalence ratio are shown in Fig. 12. It can be seen from the figure that when there is no plasma, the flameout phenomenon occurs when the equivalence ratio is 0.62; and when the plasma exists, the flameout phenomenon occurs when the equivalence ratio is 0.34. Here, the increase in the concentration of active particles O and OH produced during PAC can speed up the chemical reaction of kerosene combustion, release more heat, improve the combustion efficiency of aviation kerosene combustion, and expand the blowout boundary. A broadening of the flammable range is observed with increased applied power, as depicted in Fig. 13. Here, the flammable range is considered as the equivalence ratio range where a visible flame is observed. For an applied power of 390 W, the upper flammability limit is 2.2. This limit is 1.6 times greater than without plasma. The broadening of the flammable range is a known result in plasma-assisted combustion, and generally attributed to the “extra” energy supplied to the mixture by the plasma. Such thermal effects can be predominant in gliding arc discharges. In addition, some chemical effects could be considered, for example, hydrocarbon cracking and the NO_x catalytic effect and production in the discharge [65].

In order to investigate the ignition and LBO limits of gliding arc plasma fuel injector (GAPFI) with plasma on and off, the GAPFI is ignited with gliding arc discharge to obtain stable flame which

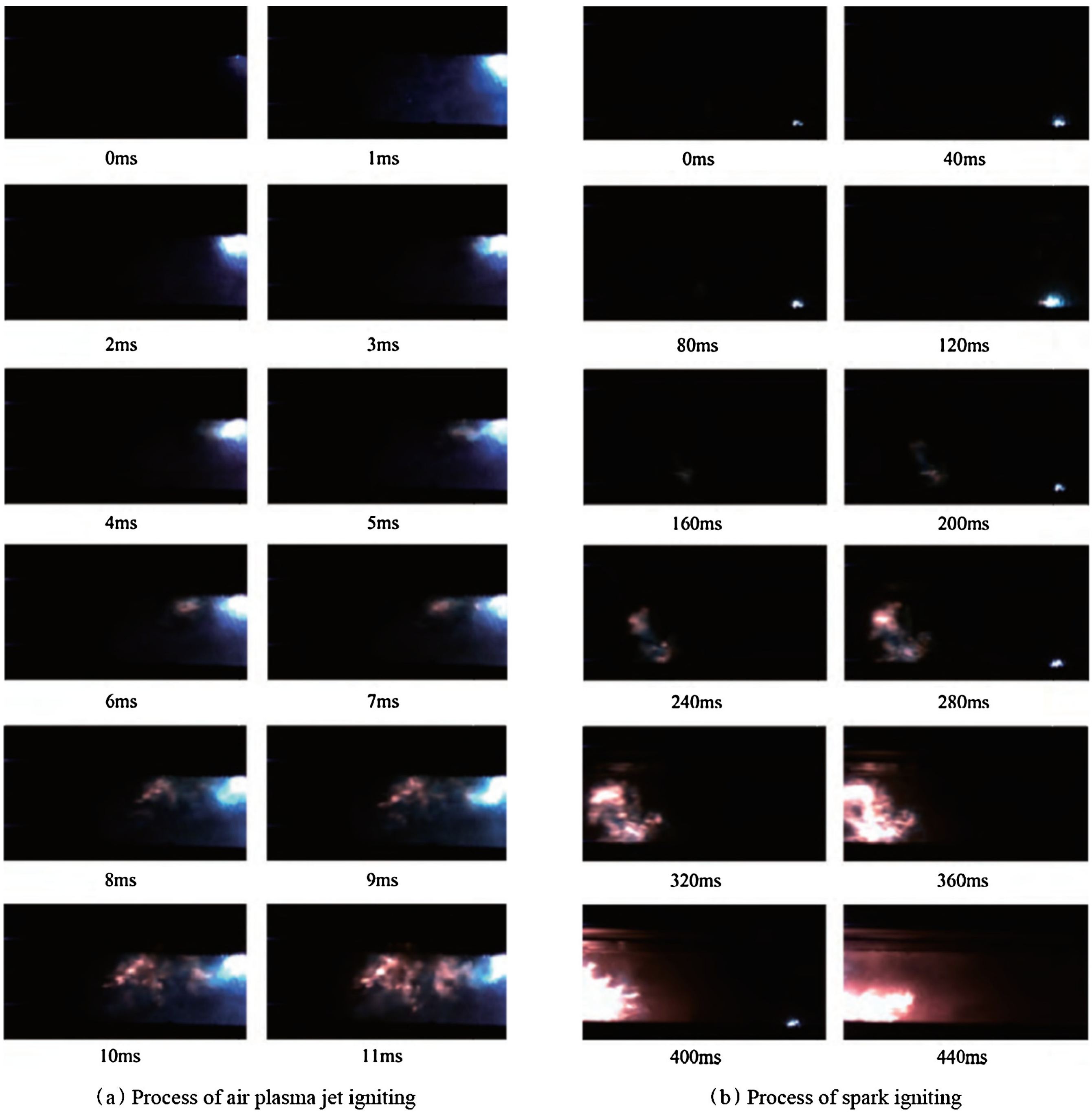

Fig. 8. Differences between plasma ignition and electric spark ignition. The inlet air velocity in the combustor is 15 m/s, the kerosene flow rate is 0.816 L/min, the working medium air flow rate of the Air Plasma Jet Igniter is 60 g/min, and the output current of the ignition drive power is 25 A. The output voltage of the electric spark igniter driving power is 27 V. Reproduced from [64].

can last for 5 s; the gliding arc discharge is then turned off to test the combustion stabilization. As shown in Fig. 14, the fuel-lean ignition limits of GAPFI with plasma are extended near the LBO boundary using 5 °C and −30 °C kerosene. This means GAPFI can not only extend the LBO limit but also improve the ignition to flame transition without an extinction limit within the plasma-assisted flammable envelope [52].

Fig. 15 shows the LBO boundary map, and the area above the LBO limit is the stable swirl flames area. When the equivalence ratio is greater than that of LBO boundary, the swirl flame can maintain stable combustion; when the equivalence ratio is less than that on the LBO boundary, swirl flame extinguishment will occur. PAC can keep the flame burning stably, indicating that the plasma can broaden the LBO boundary. The LBO limit provides a clear boundary that separates the area maintaining the flame through the vortex stabilization from that in which the frame cannot be stabilized by vortex but requires a plasma discharge to stabilize.

Fig. 16 shows the variations of the LBO equivalence ratio with the airflow rate. In the absence of plasma coupling, LBO is highly dependent on the airflow rate; in the presence of plasma coupling, LBO is only dependent on coupled plasma power, and has nothing to do with the airflow rate. Fig. 16 also shows that with the increase of plasma power, the LBO boundary becomes wider, and the LBO at each power is significantly lower than that without plasma.

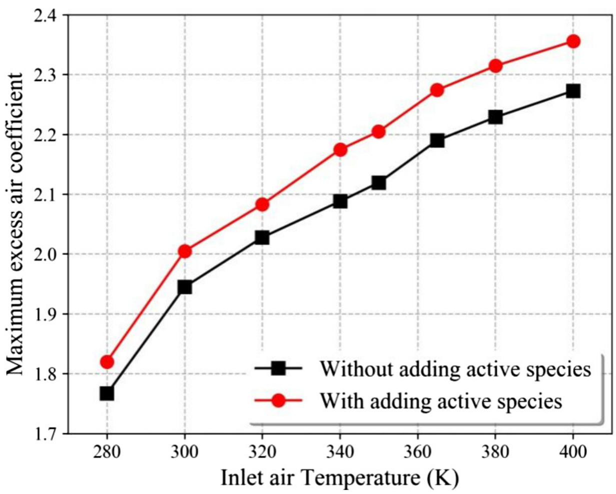

Fig. 9. Ignition boundary comparison. The plasma ignition system is composed of the plasma ignitor, high voltage power source, and cable. To obtain a large ignition kernel, several holes in the cathode wall and a unique structure for the anode are designed. Reproduced from [51].

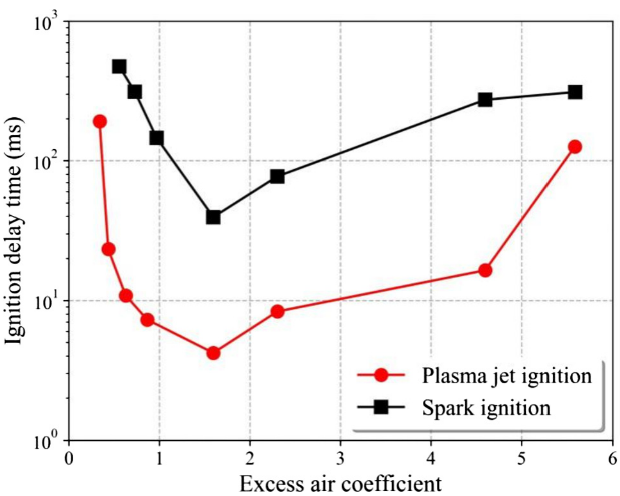

Fig. 10. Ignition delay time in spark ignition and plasma jet ignition. The average arc discharge voltage is 120 V, and the average arc current is 22 A, so the power of the plasma ignition system is 2.64 kW. Reproduced from [38].

3.4. Combustion efficiency

Combustion efficiency is used to measure the completeness of the conversion of chemical energy of fuel into thermal energy [96]. The higher the combustion efficiency, the higher the fuel utilization rate. Plasma-assisted ignition and combustion have a significant impact on the combustion efficiency of the combustor. Fig. 17 shows the combustion efficiency of conventional combustion and PAC. PAC has higher combustion efficiency than CC under varying working conditions. Plasma discharge concentrates the energy in an instant release, which increases the excitation intensity, produces an instantaneous sharp rise in temperature and pressure in the discharge area, and causes strong disturbances in the flow field. As a result, the mixing of fuel and air is enhanced, thereby increasing the contact area between the flame front and fresh mixture and achieving the goal of “transportation enhancement”.

Fig. 18(a) shows the influence of voltage and repetition rate (RR) on combustion efficiency. The combustion efficiency was not a strong function of the RR and voltage. However, due to the highly non-equilibrium temperature characteristic of the nanosecond pulsed plasma discharge (NSPD), the increase of combustion efficiency could be significant and on the order of 10% [69].

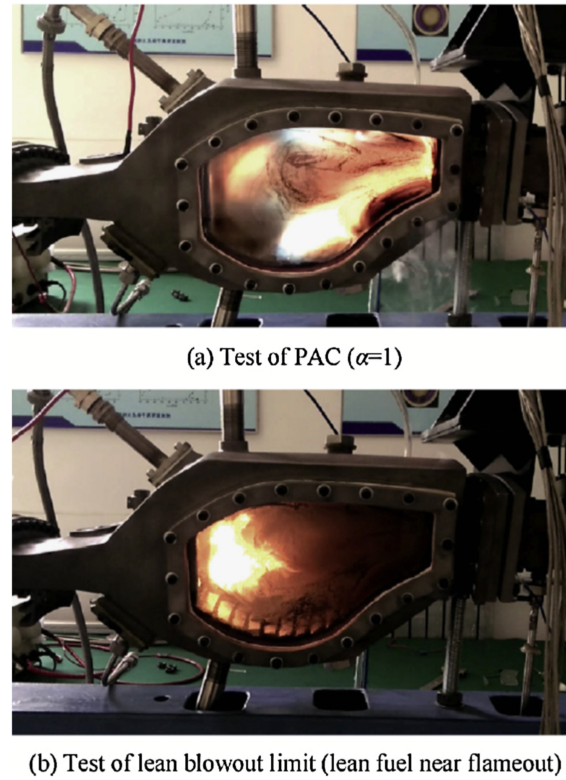

Fig. 11. Photos of the combustor in experiments. A rotating gliding arc discharge was employed to the PACA, the discharge is driven by a sinusoidal plasma power (CTP-2000S, Suman Electronics) with a frequency of 5–25 kHz, a modulation frequency of 100 Hz to 1000 Hz, a maximum peak-to-peak voltage of 30 kV, a duty ratio of 10% to 99%, and a maximum output power of 500 W. Reproduced from [53].

Fig. 18(b) shows the effect of actuator position on combustion efficiency with different combustor excessive air coefficients. Firstly, combustion efficiencies of normal combustion with different combustor excessive air coefficients increased when Plasma-Assisted Combustion Actuators (PACAs) were moved from secondary air holes to dilution air holes. Atomized liquid kerosene in the primary combustion zone could not be completely burned, and a portion of unburned fuel would enter the mixing region. Secondary combustion reactions occurring in the mixing region were intensified when fresh air was introduced into the combustor through dilution air holes, which led to the combustion efficiency enhancement [50].

In swirl combustion, the swirl number is used to describe the strength of the swirl, which represents the aerodynamic characteristics of swirling jets. When there is no plasma, the larger the swirl number is, the stronger the swirl effect and the better the mixing effect of fuel and air are, which means the higher the combustion efficiency. For plasma combustion, the combustion efficiency of the three swirling numbers is between 0.8-0.82, which is all larger than the no plasma scheme. The introduction of plasma will result in more electron collision and significantly improve the combustion efficiency. Fig. 19 suggests that the improvement with NSPD is comparable if not better than the effect of increasing SN.

Generally, the central recirculation zone (CRZ) is commonly formed in the near field of the injector exit by the swirler and used to stabilize the flame. A CRZ induced by the dielectric barrier discharge (DBD) plasma actuation was observed in the low swirl burner configuration (while there is no CRZ with DBD actuation off), as shown in Fig. 20, which clearly demonstrated that the mechanism of the combustion control by the plasma swirler is mainly through the aerodynamic effect [97]. Although the above paper only studied the variation of the CRZ flow fields and did

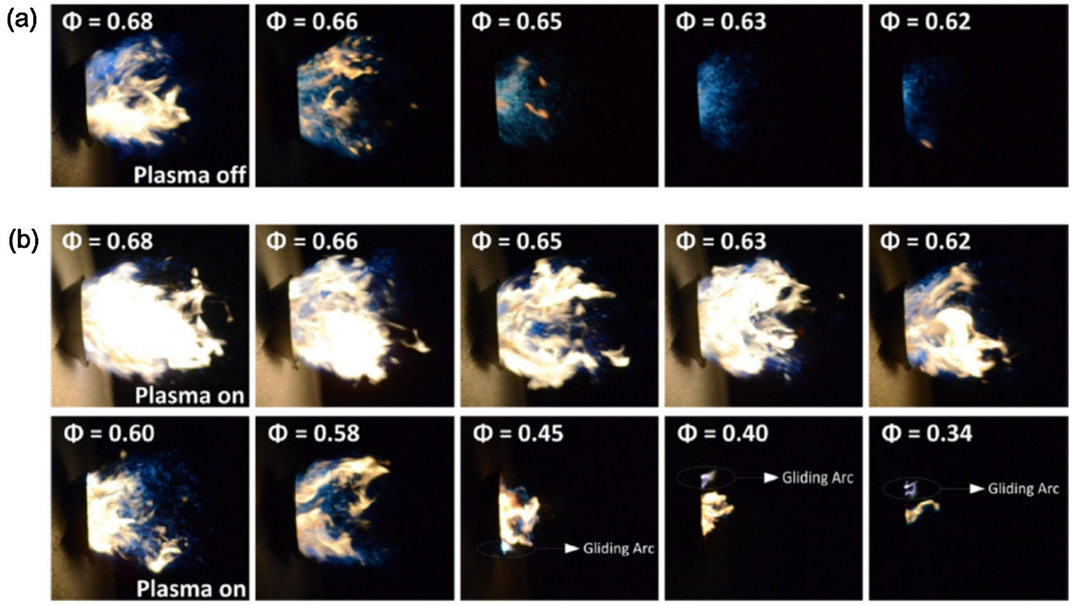

Fig. 12. Sequential images of flame: (a) with plasma off and equivalence ratio decreasing to 0.62; (b) with plasma on equivalence ratio decreasing to 0.34. The effect of GAPFI at the air flow velocity of 4.38 m/s with 5 °C kerosene is taken for example. Reproduced from [52].

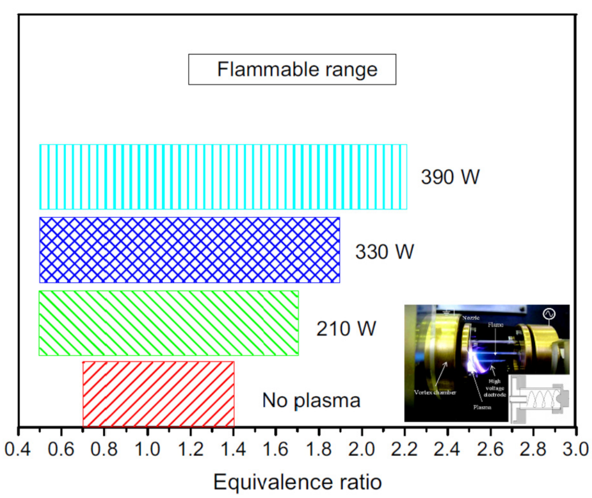

Fig. 13. Flammable range of air–natural gas flow for different applied power. Image of the plasma reactor with plasma-assisted combustion: equivalence ratio of 1.4 and r.m.s. power of 395 W. Electrical-to-thermal power ratio of 12.3%. On the bottom at right, a scheme of the reactor. The discharge (purple) is limited to the region between the nozzle and the first turn of the helical electrode. The flame (blue) is stabilized in the central axis. Reproduced from [67].

not carry out in-depth research on combustion performance (especially the combustion efficiency and NO_x), we can predict that the CRZ achieved by plasma can increase the fuel residence time in the combustor, thus promoting complete combustion of fuel. As a result, combustion efficiency is significantly improved. In the meantime, it should also be noticed that the increased high-temperature gas residence time is of no good for NO_x.

3.5. Emissions

In recent years, the International Civil Aviation Organization (ICAO) has formulated a number of emission standards to regulate the emission of pollutants from civil aviation engines, which include smoke, CO, NO_x, and HCs [98]. The emission standards for NO_x in particular have become increasingly stringent. The Annex 16 of the Chicago Convention promulgated by the ICAO stipulates the standard landing and take-off cycle (LTO), which is divided into four stages: taxi, take-off, climb, and approach, as shown in Fig. 21. Different amounts of emission are allowed in different stages.

Different countries have developed plans to fabricate high-performance and low-emission aerospace engines to reduce pollutant emissions and meet the increasingly stringent environmental protection regulations. Many low emission combustion technologies and novel combustors have been developed, such as Lean Premixed Prevaporized (LPP) [100–103], Lean Direct Injection (LDI) [104–108], Rich-Quench-Lean (RQL) [109–113], staged combustion technology and Twin Annular Premixing Swirler (TAPS) combustor [114–116], Trapped-vortex Combustor (TVC) [117–124], etc., as shown in Fig. 22.

The reduction of pollutants can be achieved by PAI and PAC technology, indicating that it is a good prospect in the field of low-pollution combustion. Researchers have carried out a comparison of emissions between plasma and conventional ignition, and the results show that after the plasma is turned on, pollutant emissions can be significantly reduced [56,78,82], as shown in Fig. 23 and Fig. 24.

As shown in Fig. 25, after the implementation of plasma-assisted combustion, the region with a higher CO volume fraction is located in the main combustion zone of the combustor and it is significantly reduced in the downstream mixing zone. With the PAC, the CO volume fraction level at the exit position is significantly lower than that in the normal combustion state without plasma-assisted technique, indicating that the active particles participate in the chemical reaction of combustion in the main combustion zone to accelerate the combustion reaction and promote the full combustion of the fuel, so that the incompletely burned fuel remaining at the outlet is significantly reduced. Kim et al. performed research on the influence of plasma on NO_x emissions (Fig. 26) [69], showing that NO_x production is a linearly increasing function with the applied voltage and plasma repetition rate.

3.6. Outlet temperature of combustor (OTDF/RTDF)

An important development trend of aero-engine combustors is high-temperature rise, and the quality of outlet temperature is one of the important performance indicators of aero-engine combus-

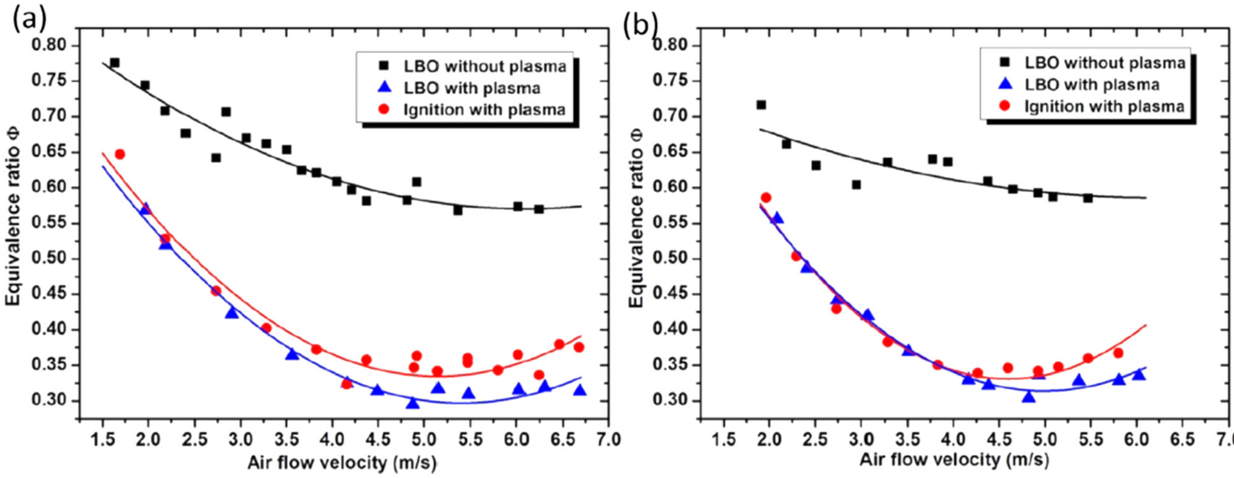

Fig. 14. Effect of plasma on the ignition and LBO limit using GAPFI with (a) 5 °C and (b) −30 °C kerosene. For the gliding arc plasma system, the steel fuel atomizer acts as a high voltage electrode and the steel venturi nozzle is connected to the ground as an outer electrode. The plasma reactor is powered by a high voltage power supply (CTD-1000Z) allowing a maximum voltage of 20 kV and rated power of 2000 W with AC discharge. Reproduced from [52].

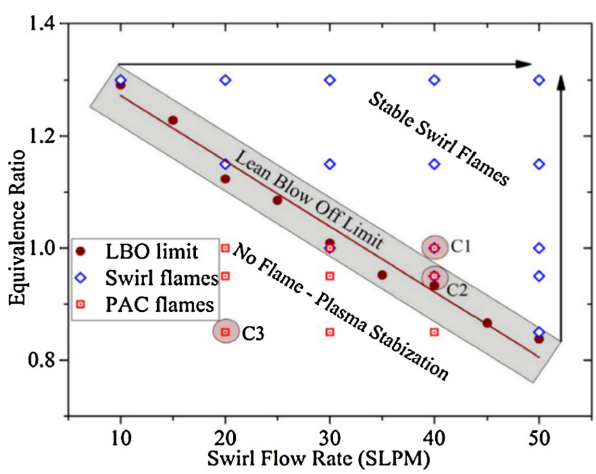

Fig. 15. LBO Boundary. Plasma power: black-0 W, red-35 W, blue-50 W, green-100 W, and violet-120 W. Open: swirl flames. Dot: PAC flames. Reproduced from [66].

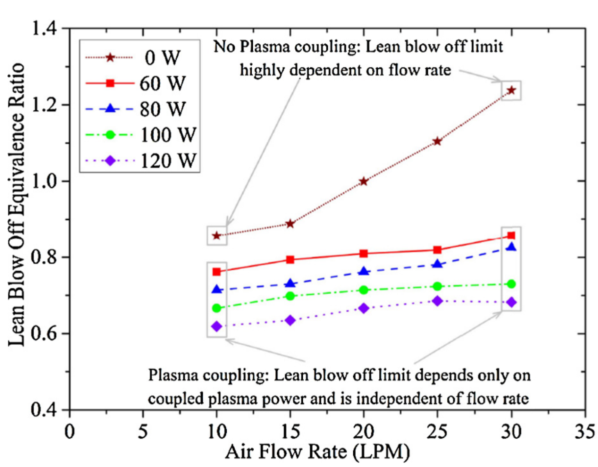

Fig. 16. LBO equivalence ratio versus the airflow rate with/without plasma. Direct microwave plasma coupling was employed in this study. The swirl flow rate is 40 standard liters per minute (LPM). Reproduced from [67].

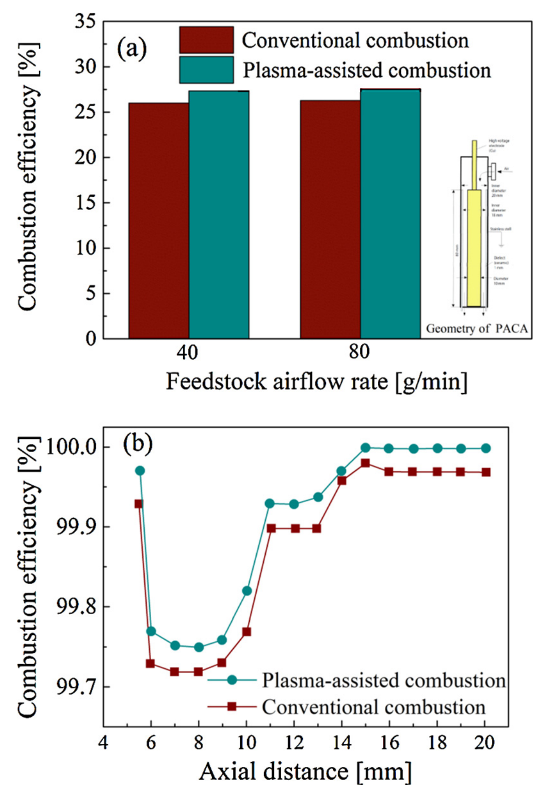

Fig. 17. Combustion efficiency of conventional combustion and plasma-assisted combustion. (a) The discharge was driven by a sinusoidal plasma power supply with a frequency in the range from 5-25 kHz, modulating the frequency of 100-1000 Hz, a maximum peak-to-peak voltage of 30 kV, the duty ratio of 10-99%, and output power of 500 W, and (b) The initial electron temperature is set by 5 eV, CH4-air mixtures temperature is 300 K, the pressure is 101325 Pa, the inlet velocity is 10 m/s, a high-frequency sinusoidal voltage is applied to the two electrodes. Reproduced from [50] and [56], respectively.

tors [125–127]. In particular, the outlet temperature distribution and hot spot temperature play a decisive role in the performance, life, and reliability of turbine components. The inhomogeneity of the outlet temperature field must be reduced to ensure that the turbine can operate normally in high-temperature and extreme environments. With the continuous improvement of modern aero-engines quality of the outlet temperature of the combustor, the research on the characteristics of outlet temperature distribution has also attracted more and more attention. A series of studies have investigated the effect of PAC in the combustor. The results show that the temperature distribution of the combustor is improved when the PAC is employed.

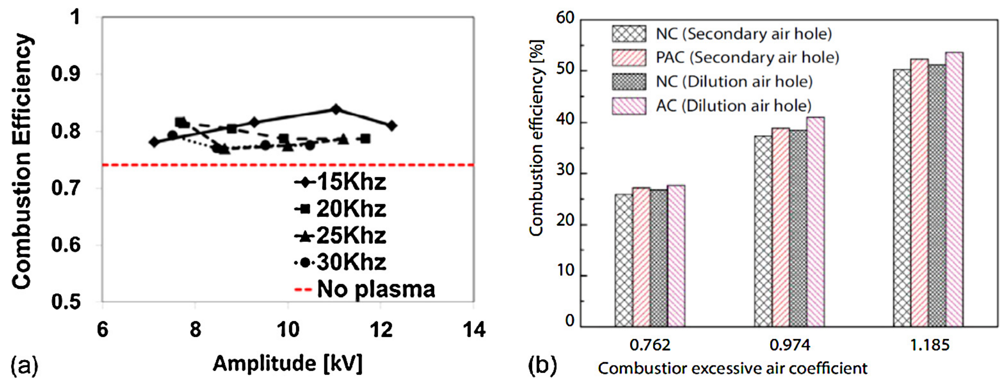

Fig. 18. (a) The influence of the voltage and power on the combustion efficiency with (black) and without (red) the nano-second pulsed plasma discharge, reproduced from [69]; (b) the effect of the actuator position on the combustion efficiency with different combustor excessive air coefficients, reproduced from [50].

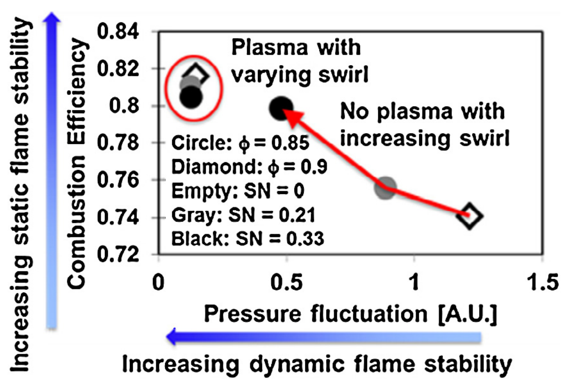

Fig. 19. Increasing the operability limit by using NSPD. In the presence of the NSPD (red circle), the static flame stability is increased by ∼10% and, simultaneously, the dynamic flame stability is improved by 10× in comparison to data without NSPD (empty diamond outside of the red circle). Reproduced from [69].

In general, the outlet overall temperature distribution factor (OTDF) and the outlet radial temperature distribution factor (RTDF) are two common indices to measure the outlet temperature distribution of the combustor. OTDF refers to the ratio of the difference between the highest total temperature and the average total temperature of the combustor outlet section to the total temperature rise of the combustor; RTDF is defined as the ratio of the difference between the highest average total radial temperature (which is calculated by taking the arithmetic average in the circumferential direction on the total temperature of each point on the same radius of the combustor outlet section) and the average total outlet temperature to the temperature rise of the combustor.

Experiments have found that with the implementation of PAC, the fuel is combusted as completely as possible in the upstream main combustion zone [45]. In the downstream mixing zone near the exit of the combustor, secondary air is added to mix with the high-temperature gas uniformly, so that in PAC operating conditions the degree of nonuniformity of the outlet temperature field is smaller and the outlet temperature field is more uniform than normal.

A Plasma-Assisted Combustion (PAC) test platform was developed to validate the feasibility of using PAC actuators to enhance annular combustor performance. Two plans of PAC (using rotating gliding arc discharge plasma) were designed, Assisted Combustion from Primary Holes (ACPH) and Assisted Combustion from Dilution Holes (ACDH). The OTDF and RTDF of the two plans can be seen in Fig. 27. For ACPH, its OTDF and RTDF reach 0.3271 and 0.1243 respectively when α is 1 and U_0 is 0 V, while its OTDF and RTDF decrease to 0.3119 and 0.1196 respectively when U_0 is 120 V. For ACDH, PAC decreases its OTDF and RTDF from 0.3368 and 0.1338 to 0.3289 and 0.1325, respectively [53].

The effect that improves the OTDF of ACPH is more obvious than that of ACDH. On one hand, the fuel burns as completely as possible in the main combustion zone, and high-temperature gas is sufficiently far away from the combustor outlet to mix well. On the other hand, it may be due to supplying air from primary holes and dilution holes, which affects the original combustion in the flame tube. The dilution holes are closer to the outlet of the combustor, and the negative factor of additional air supplying affects combustion more obviously than that in Plan A. It is clear that the pattern factor of ACPH is more uniform and suitable for this combustor than that of ACDH, but the PACA in the two schemes only decreases the RTDF slightly [53].

Dielectric barrier discharge (DBD) plasma is a non-equilibrium plasma, which has the advantages of a large available pressure range, high reliability, small volume, etc. It is often used to design plasma-assisted combustion actuators (PACA) that can be applied to the combustor of aero-engines. The charged particles (electrons and ions) move in DBD region and transfer momentum and energy to neutral particles, which will enhance active particles transport, form plasma vortexes and turbulence, generate active species, accelerate chain reaction or create new chain reactions, and result in an increase of the combustion efficiency. Usually, different types of DBD PAC actuator are used to improve the performance of engines. Deng et al. designed a parallel plate DBD PAC actuator for improving the reverse-flow combustor of a small realistic turboshaft aero-engine, with the results indicating that the engineering application of DBD PAC is feasible on the small combustor of aero-engine [49]. The OTDFs of PAC and CC are shown in Fig. 28. The uniformity of the outlet temperature distribution is generally improved by using PAC. The percent decrease in the OTDFs between PAC and CC was 11.1%-26.6%.

3.7. Combustion stability/oscillating combustion

Combustion oscillation is a manifestation of unstable combustion [128]. In this phenomenon, the combustion parameters fluctuate violently when the relationship between the internal sound pressure in the combustor and the heat release reaches a certain phase, and the parameters strengthen each other. On the one hand, this oscillation can promote fuel-air mixing, enhance the mixing effect, and facilitate the combustion in the combustor; on the other hand, it will cause additional high-amplitude oscillations of pressure, flow field, and flame, increase the thermal load, aggravate the production of pollutants, affect the normal operation of the combustor, and in serious cases would cause damage and destruction of system components.

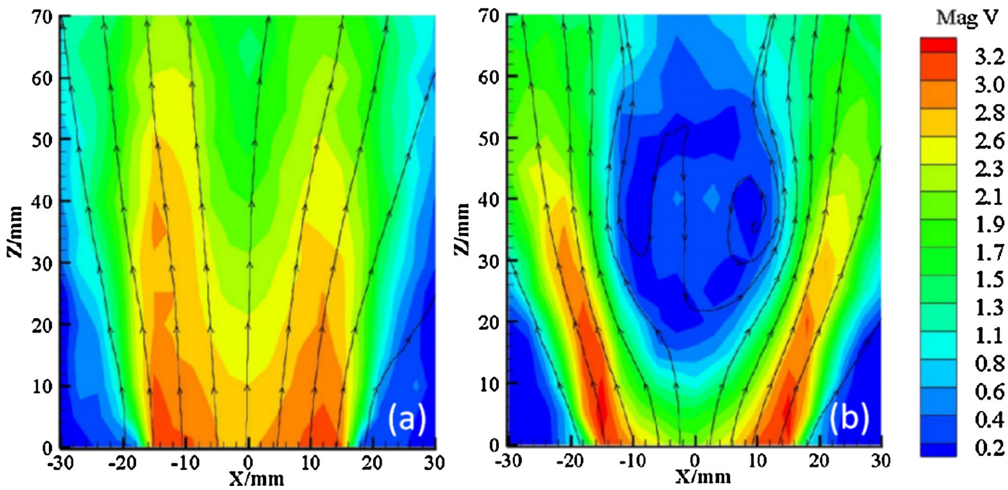

Fig. 20. Non-reacting streamlines and velocity magnitude contours obtained by Laser Doppler Anemometry (m/s) with the air volumetric rate at 162 L/min. (a) DBD actuation off and (b) DBD actuation on (15 kV). Reproduced from [97].

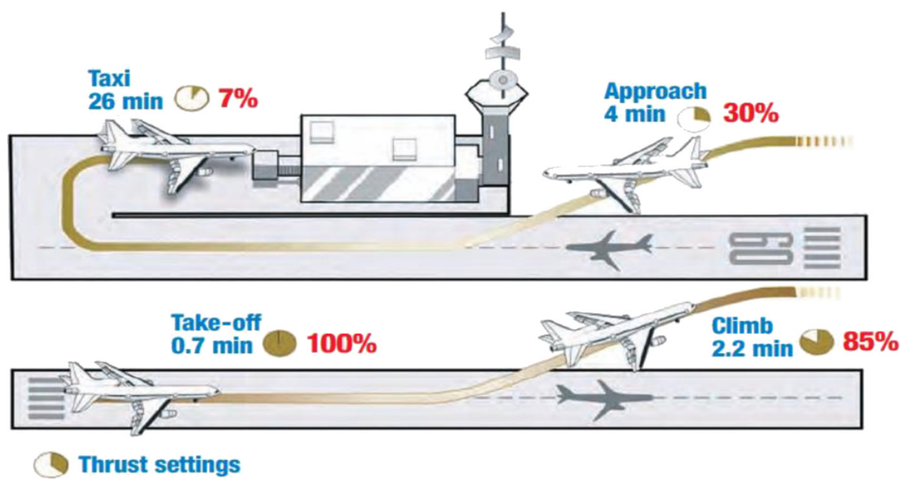

Fig. 21. Illustration of the ICAO Emissions Certification Procedure in the LTO Cycle. Reproduced from [99].

As a new type of active control method in recent years, plasma has distinct advantages compared to traditional control methods: short delay, no moving parts or other complex structures, lower energy consumption, and fewer pollutants; the associated thermal and chemical effects can significantly affect the combustion processes [129]. In recent years, experimentalists have found that plasma can stabilize the flame, thereby slowing down the combustion oscillation. Using plasma to control combustion oscillation in the combustor has emerged as a valuable research topic.

Moeck et al. integrated nanosecond pulse discharge into the swirling combustor [75]. It was found that the nanosecond pulse discharge can significantly affect the flame shape under certain conditions, and when the repetition frequency changes, the flame shape will also be changed, accordingly. They also found that adding nanosecond pulses under different conditions may reduce oscillation in the original system (Fig. 29(a)) and may also make the system change from a stable state to unstable oscillation (Fig. 29(b)).

Rajasegar et al. investigated the reduction in flame dynamics during plasma discharge. It was found that plasma strengthening can reduce pressure fluctuations [66]. To further support the reduction in flame dynamics in the presence of plasma discharge, the overall root mean square (RMS) value of the pressure fluctuations (frequency integrated) for the three configurations is shown in Fig. 30. The plasma discharge results in a significant reduction in the pressure fluctuations in all the test cases. C1-P and C2-P showed an overall reduction of about 42% and 47% in RMS pressure fluctuations when compared against their corresponding baseline cases C1 and C2 even for the minimum plasma power addition of 35 W. This also supports the idea that nonthermal effects of the plasma discharge allow for stronger plasma-flame coupling at leaner equivalence ratios. It is also observed from test case C3-P that a progressive increase in the plasma power actually over-energizes the flame, resulting in an undesirable increase in the RMS pressure fluctuations.

Kim et al. studied the effects of nanosecond-pulsed plasma on noise, heat release rate, pressure and other parameters when self-excited oscillations occur in the combustion system and proposed a mechanism of oscillation reduction through nanosecond-pulsed plasma [69]. They believe that for a sudden expansion of combustor, the combustion zone can be divided into two areas: the central zone (CZ) and the outside recirculation zone (ORZ). The CZ is less affected by flow disturbances, where the flame undergoes relatively gentle combustion; the ORZ is greatly affected by the vortex shedding, where the burned flame will produce larger oscillations. The appearance of nanosecond-pulsed plasma changes the shape of the flame to stabilize the combustion in the CZ, greatly slowing down the oscillation amplitude and suppressing the combustion oscillation phenomenon. The NSPD changed the shape of the flame inside the combustor, and the base of the flame did not move, the oscillating pressure fluctuations of the combustor could be reduced significantly.

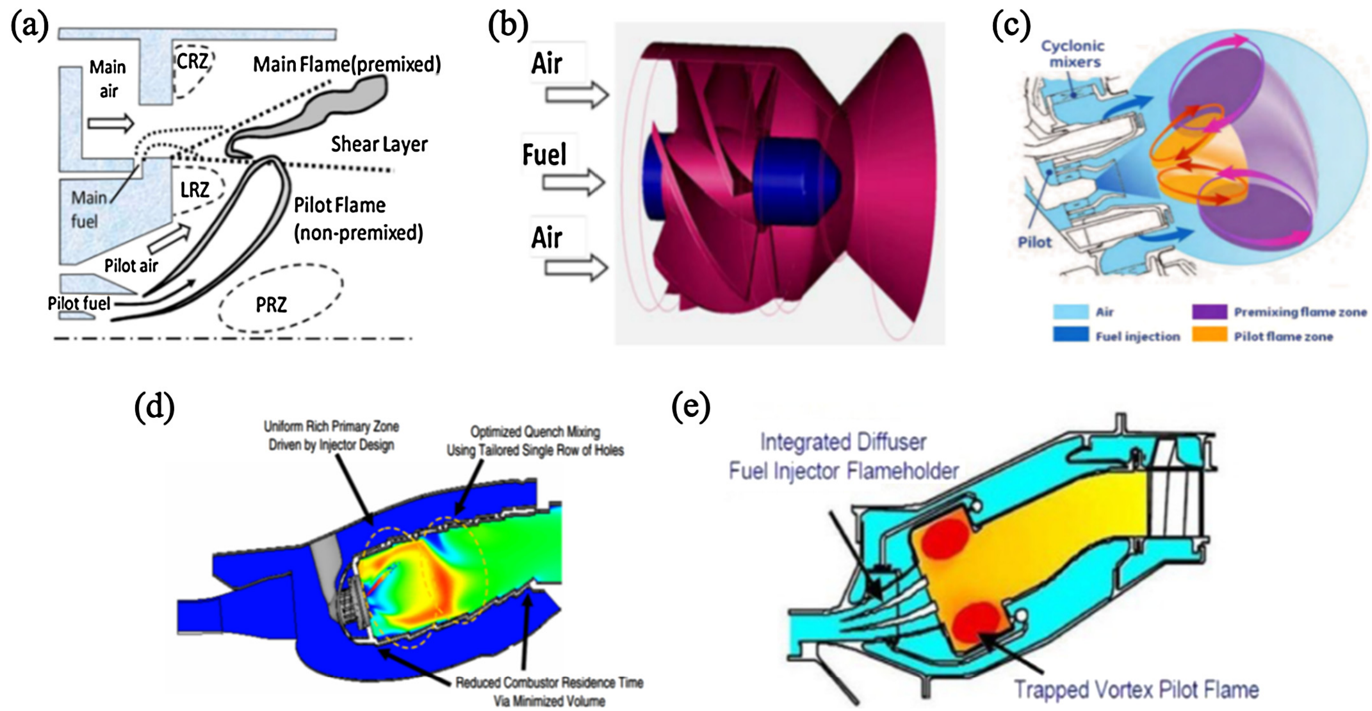

Fig. 22. Potential combustion technologies with low emission: (a) LPP [100], (b) LDI [104], (c) TAPS [115], (d) RQL [112], and (e) TVC [120].

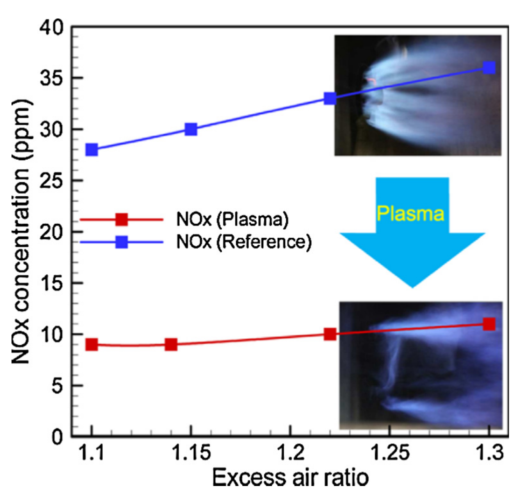

Fig. 23. Plasma-assisted combustion technology for NO_x reduction. 50-150 W of power was used to generate plasma, a value less than 0.1% of the fuel heating value. Reproduced from [78].

3.8. Fuel reforming

The effect of plasma on fuel spray is presented in Fig. 31. The results show that the drop sizes of kerosene spray further decrease via the gliding arc plasma effects of GAPFI. The ignition limit and lean blow-out limit were largely extended. The effects of GAPFI in fuel reforming are examined in reference [52]. The typical detected reforming products in gas stages are presented in Fig. 32. During gliding arc discharge, a large number of active radicals (e.g., N_2, O_2, NO, N_2^+, N, NH, O, and OH) are generated by electron impact dissociation, collisional dissociation and recombined dissociation effects. These electrons, ions, molecules, and active species with high energy actively participate in splitting the C-H bond and C-C bond of hydrocarbon macromolecules of kerosene during collisions and contribute to the dissociation of hydrocarbon macromolecules into light ones with carbon number less than 5. As shown in Fig. 32, products detected at the gas stage include methane (CH_4), ethane (C_2H_6), ethylene (C_2H_4), acetylene (C_2H_2), propane (C_3H_8), propylene (C_3H_6), allene (C_3H_4), propyne (C_3H_4), and butane (C_4H_8) (including three isomers: 1-butene, isobutene, and 1,3-butadiene). Amongst these, CH_4 (1.26 SLM), C_2H_4 (1.31 SLM), and C_2H_2 (2.30 SLM) are the major products. These light hydrocarbons have larger laminar flame propagation velocities and are easier to be ignited at low temperatures, especially for olefins.

The fuel atomization effect can be more distinct by utilizing the cracking effect of plasma, which can help improve the uniformity of the fuel and air mixture, generate active particles that promote the combustion chemical reaction, and thus solve the problems of the aero-engine under special conditions [12,26,91]: slow ignition speed, long ignition delay time, low combustion efficiency, lean fuel flameout, high-altitude ignition, and nonuniformity in temperature field at the exit of the combustor. Its features include cracking fuel efficiently, assisting fuel atomization, generating a large number of active particles, simple structure, and strong versatility.

A large number of high-energy electrons and active particles generated during the plasma discharge collide with the atomized small fuel molecules, and the bonds between the high-carbon fuel molecules are broken, forming low-carbon small molecules with a lower "boiling point" [130]. On the one hand, the process of discharging fuel oil can generate such low-carbon small molecules, which participate in the combustion in the form of gaseous fuel and thus can accelerate the process of combustion and flame propagation, and improve the completeness of combustion; on the other hand, the active particles generated in the discharge process, such as oxygen atoms, ozone, ions, and active groups, participate in the combustion reaction, increasing the rate of the chemical reaction of combustion. Besides improving the combustion efficiency, it also widens the range of stable combustion and LBO boundary, improves the quality of the outlet temperature field, and reduces pollutant emissions.

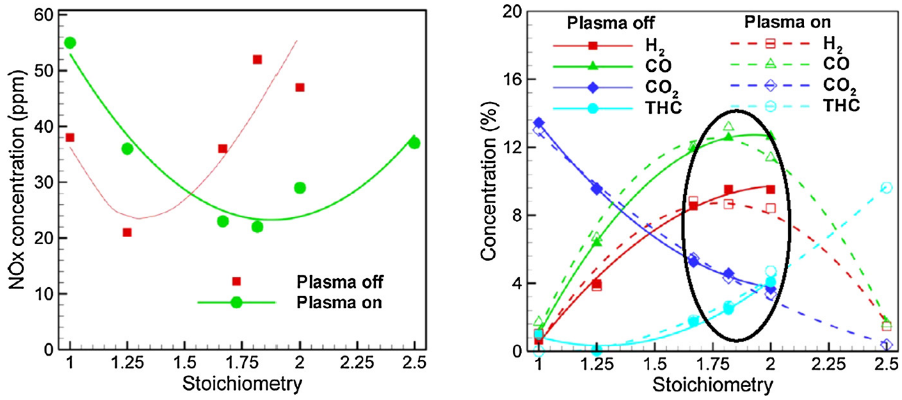

Fig. 24. The generation of NO_x, CO, and THC are compared with and without plasma. A total of 150 W of power was used for the generation of plasma. Reproduced from [82].

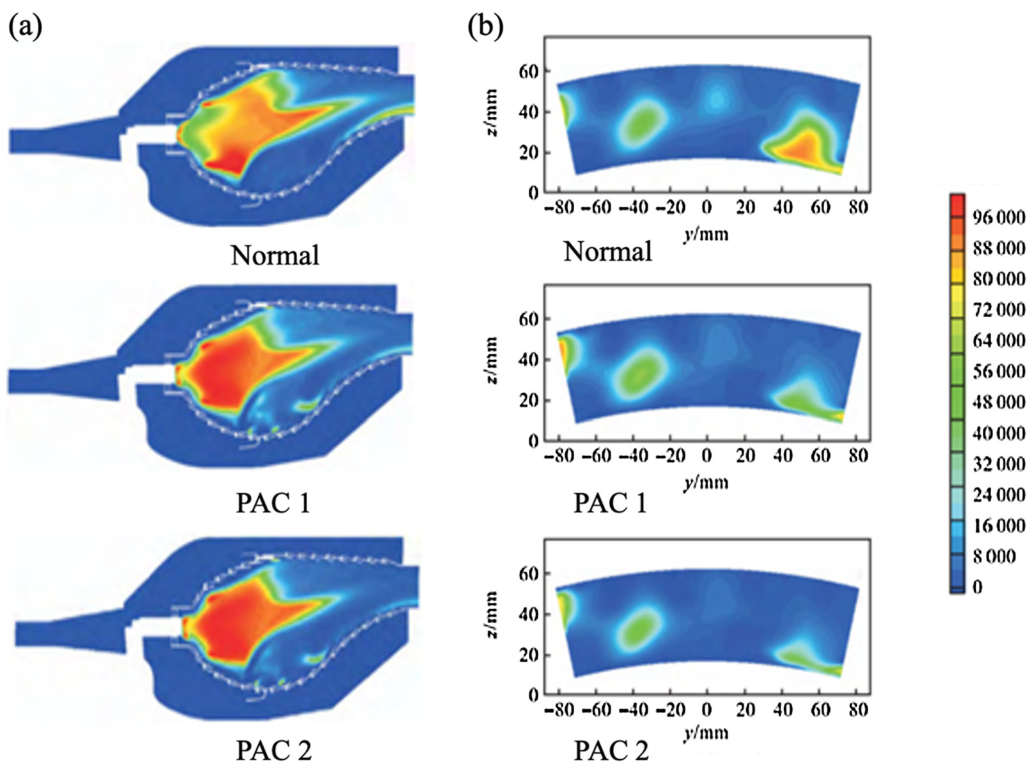

Fig. 25. Numerically calculated CO concentration distribution for PAC and normal combustion schemes (the excess air coefficient equals one): (a) observed cross-section and (b) cross-section at the exit. Reproduced from [47].

4. Application of plasma in the new aerospace engine combustor

With the development and gradual maturity of PAI and PAC technology in aerospace engines, the use of plasma technology, especially PAI technology, has gradually increased in several new aerospace engines [131]. The utilization of PAI technology in aerospace engines has many advantages, including accelerating the physical and chemical process of fuel and oxidant combustion, expanding the ignition concentration limit, increasing the flame propagation speed, and significantly improving the ignition reliability and combustion stability. Furthermore, plasma can be reused multiple times in engines that require multiple starts and is an ideal choice in the engine development stage.

4.1. Powder engine

A powder engine is an engine fuelled by metal or other high-energy powders [132]. It has the advantages of insensitivity to temperature, good long-term storage, and strong environmental adaptability. It also can be started multiple times, and the thrust is adjustable. Powder engines with different fuel/oxidant combinations can be used in different situations by adopting different fuel/oxidant combinations. Two of the most representative powder engines are the Al/AP powder engine and Mg/CO_2 powder engine [133,134]. The Al/AP powder engine takes Al powder as fuel and AP as oxidant. It is suitable for tasks that require long-term storage, multiple starts, and adjustable thrust, such as an attitude orbit control engine. The Mg/CO_2 engine takes Mg powder as fuel and liquid CO_2 as oxidant. The Mg/CO_2 powder engine is planned for use in rockets for Mars exploration tasks because liquid CO_2 can be obtained from and produced on Mars to reduce the cost of Mars exploration missions.

In the above-mentioned two powder engines, the processes of AP decomposition in the Al/AP engines and the gasification of the liquid carbon dioxide in the Mg/CO_2 engines consume a considerable amount of heat, causing difficulties during ignition due

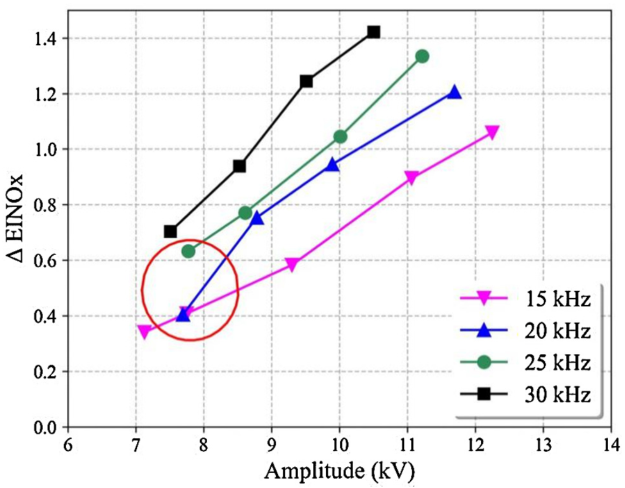

Fig. 26. Incremental NO_x in the presence of NSPD, where $EINO_x$ is defined as grams of NO_x produced per kg fuel consumption. Although it is clear that the NO_x production is a linearly increasing function with the applied voltage and plasma repetition rate, the $EINO_x$ increase was minimal and around 0.5EI for the typical range of NSPD used in the current study (red circle). Reproduced from [69].

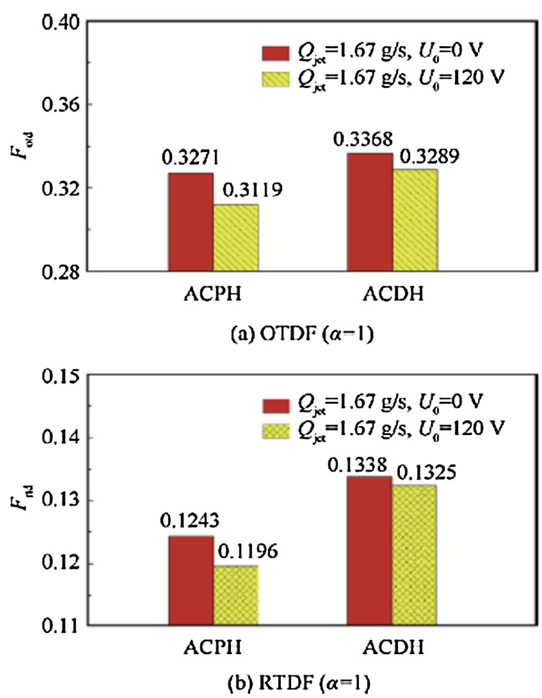

Fig. 27. Effect of ACPH/ACDH on the temperature field distribution of the outlet. U_0 is 0 V in a normal condition, while in a PAC condition, U_0 is 120 V. In order to verify the effect of PAC and eliminate the interference of additional air feed by PACAs, the jet flow rate (Q_{jet}) is 1.67 g/s in all test conditions. Reproduced from [53].

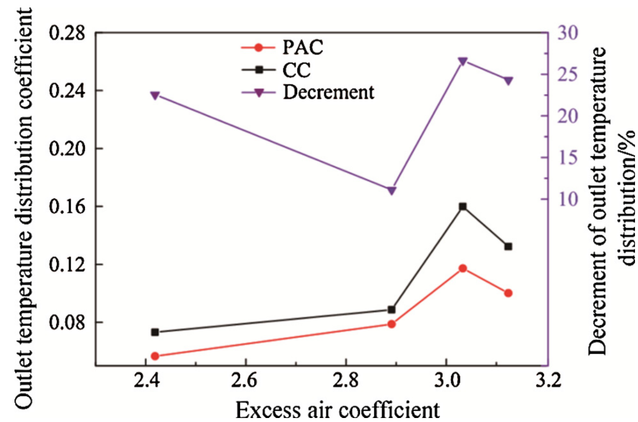

Fig. 28. OTDF and their decrements of CC and PAC. A parallel plate double DBD PAC actuator section is designed as a practical approach. The double high-voltage differential power supply (Suman Electronics, CTP-2000S, 5–25 kHz frequency range) is used to drive plasma discharge. Reproduced from [49].

to insufficient heat supply. Therefore, a powerful and reliable ignition device is required to achieve multiple ignitions at different flow rates. In the traditional scheme, one ignition engine is used only for ignition. This solution has several problems, such as difficulty in aligning the multiple start sequence, heavy structures, high ignition peak, and significant tailing [136]. Therefore, Li et al. proposed a plasma igniter for the Mg/CO_2 powder engine, as shown in Fig. 33 [135]. When the PAI start method is used in the rocket engine, the powder-powder combustion form is transformed into a partially active ion-powder combustion form. This configuration substantially reduces the difficulty of engine ignition and avoids the deflagration of the combustor caused by multiple starts and uneven mixing of the powder fuels and oxidizers, thereby improving the safety and convenience of engine ignition under various working conditions [136]. In the test, the plasma igniter showed good performance and stability during multiple ignitions, meeting the ignition requirements of powder engines.

4.2. Pulse detonation engine

A pulse detonation engine is an engine whose thrust comes from a continuous detonation wave with high temperature and pressure that is generated by detonation [137]. Since this kind of engine can compress gas without a compressor and other components, it has a simple structure and thus it has a lower cost, in addition to a high thrust-to-weight ratio. All of these advantages make the pulse detonation engine a very good candidate for aerospace vehicle power.

Wang et al. used a plasma igniter to ignite a pulse detonation engine. The effects of the initial conditions were evaluated, including the equivalence ratio, a temperature range of 280 K to 430 K, and a pressure range of 1 to 6 atm. Ignition delays were reduced by up to a factor of 5, and the deflagration-to-detonation time was lower than in conventional capacitive discharge systems [138].

Rodriguez et al. tested the plasma igniter system of a pulse detonation engine in a dynamic flow ethylene/air mixing combustor [139], as shown in Fig. 34. The experiments showed that the transient plasma ignition (TPI) was more effective and reliable than spark plug ignition and significantly improved the deflagration-to-detonation transition (DDT) performance. The TPI two-electrode concept proved to be the most effective configuration. Compared with the capacitor discharge spark plug configuration, the DDT distance and time were reduced by an average of 17% and 41%, respectively.

Daniel et al. developed a miniaturized PAI device [140], as shown in Fig. 35. The upper-left diagram shows a 12-ns transient plasma igniter, and the lower-left diagram shows an 85-ns transient plasma ignition. On the right is a 12-ns transient plasma igniter. The experiments showed that an ignition delay similar to previous experiments could be achieved even if a smaller electrode geometry and a lower energy level were used.

4.3. Pasty propellant

A paste engine is a new type of engine that combines the advantages of solid and liquid rocket motors. The solid propellant is

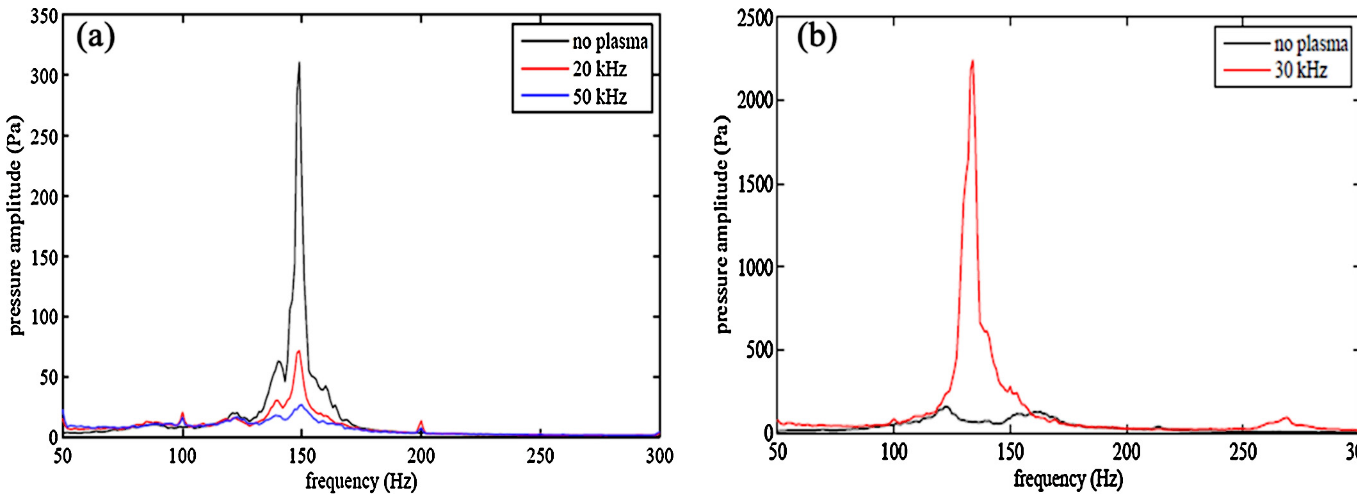

Fig. 29. (a) Amplitude spectra of the acoustic pressure measured in the combustor without and with plasma discharges at pulse repetition frequencies of 20 and 50 kHz using electrode configuration I; equivalence ratio 0.66, thermal power 43 kW. (b) Amplitude spectra of the combustor pressure without and with discharges at a pulse repetition frequency of 30 kHz, using electrode configuration I. The equivalence ratio is 0.63 and the thermal power 92 kW. Reproduced from [75].

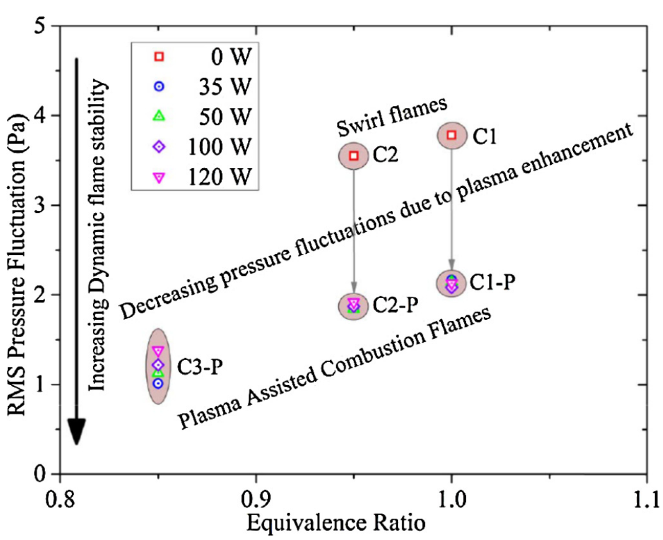

Fig. 30. Frequency averaged RMS pressure fluctuations for the three configurations for different levels of plasma power. It can be clearly seen that the plasma discharge results in a significant reduction in the pressure fluctuations in all the test cases. Reproduced from [66].

modified to have a consistency similar to toothpaste. The engine structure is simpler than that of a liquid rocket engine, and the engine is capable of multiple starts, and the thrust is adjustable. PAI has been widely used in paste engines, and an example is shown in Fig. 36 [141–143]. Zhou tested three PAIs: electric corona, electric arc, and the composite operation mode of double plasma of electric corona and electric arc [141]. He used PAIs to ignite double base pasty propellant and composite pasty propellant. The ignition delay is shown in Table 2. Zhou thought the composite operation mode of double plasma of electric corona and the electric arc was the best to use for the pasty propellant. The results showed that the ignition system has high power and good reliability. The ignition time of the composite plasma is longer than that of the conventional ignition powder, and the initial pressure peak in the ignition of the powder disappears. The PAI method can satisfy the performance requirements of the paste engine for multiple starts.

Table 2
The ignition delay of different kinds of PAI [141].

PAI	Ignition delay (ms)	
Electric corona	double base pasty propellant	Fail
	composite pasty propellant	297
Electric arc	double base pasty propellant	Fail mostly
	composite pasty propellant	Fail mostly
Composite (electric corona and electric arc)	double base pasty propellant	328
	composite pasty propellant	188

5. Prospects and challenges

5.1. Improvement in PAI and PAC technology readiness level (TRL)

Researchers conducted numerous combustor verification tests to promote the use of plasma in actual combustors. Fig. 37 shows the roadmap of the development and technological maturity of the aero-engine combustor. Currently, PAI and PAC are mostly in the TRL3-TRL4 stage, and some projects are in the design and experimental stage of the full annular combustor (TRL5). On the one hand, the use of combustor models and simplified test conditions in experiments does not fully reproduce all physical phenomena occurring in a real combustor. The parameters of the expansion combustion process at high-speed airflows vary significantly, and the influencing factors are complicated. On the other hand, there are interactions and coupling design issues between the plasma and the combustor. The choice of plasma type and the manner in which it participates in the combustion process affect the plasma performance. In addition, the ignition device in aerospace engines is generally heavy to meet the current high ignition voltage, which contradicts the requirement of being lightweight [63]. Therefore, the requirements of low weight and small size of these types of aerospace engines have not been achieved to date.

5.2. Configuration at the head of the aero-engine combustor

Currently, two main schemes exist for injecting plasma into the combustor of aerospace engines, namely, the pre-generation of plasma, which is then sprayed into the combustor liner, and the addition of a plasma combustion-supporting exciter in the combustor to generate plasma directly. In some configurations, the existing electric spark igniter is replaced by a plasma igniter, whereas in others, a combustor head based on three-dimensional rotating

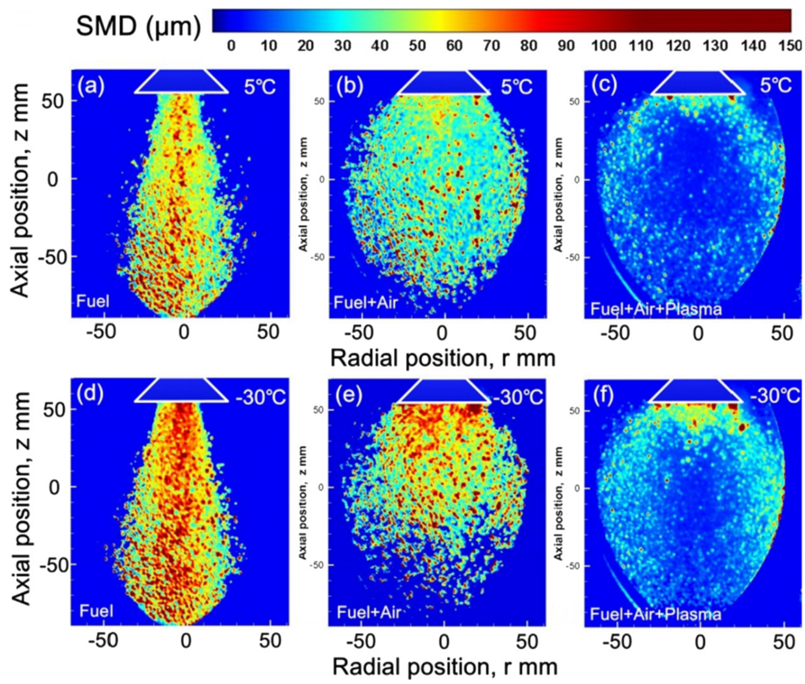

Fig. 31. Effects of airflow (250 SLM) and gliding arc plasma on fuel sprays at 5 °C and −30 °C with an injection pressure of 0.15 MPa. For the gliding arc plasma system, the steel fuel atomizer acts as a high voltage electrode and the steel venturi nozzle is connected to the ground as an outer electrode. The plasma reactor is powered by a high-voltage power supply (CTD-1000Z) allowing a maximum voltage of 20 kV and rated power of 2000 W with AC discharge. Reproduced from [52].

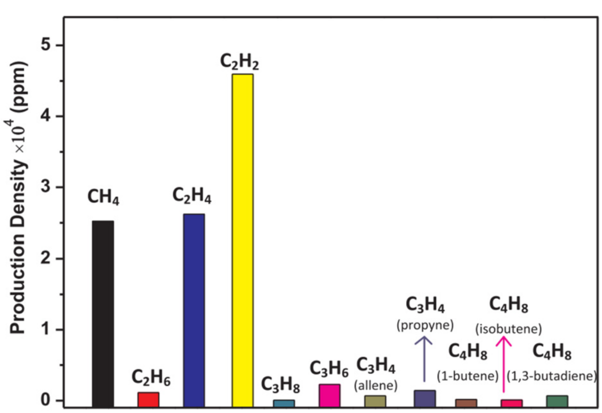

Fig. 32. The concentrations of the detected reforming products. The concentrations of detected reforming products with injection pressure at 0.11 MPa and airflow ratio of 50 SLM. Reproduced from [52].

sliding arc plasma is used (Fig. 38) [144]. In this new type of combustor head, the internal/external electrodes are configured to form the head of the three-dimensional rotating sliding arc combustor without changing the existing structure of the combustor of aerospace engines. The head of the combustor allows for PAI and PAC, taking advantage of the use of plasma for both aspects and achieving high-efficiency combustion of aerospace engines.

The advantage of a plasma-enhanced combustion dome is that the discharge position is as close as possible to the main combustion zone, and the generated active particles can participate in the combustion chemical reaction as soon as it happens, reducing the probability of active particle recombination [145]. More importantly, the atomized fuel passes through the high-energy electron zone. The fuel gas as a mixture in this region is more conducive to the ignition and combustion of the combustor, and it can be more effective and reliable under broad conditions even without the need for a traditional spark igniter on the wall of the combustor liner.

The plasma atomization nozzle designed for engineering applications of the aerospace engine combustor has to have a simple structure, strong versatility, and provide good ignition performance and fuel atomization. In addition, the PAI and PAC can only be achieved by replacing the head of the original combustor liner; thus, the structure, size, and flow distribution have to be the same as that of the original combustor. One solution proposed in Ref. [144] is that the swirling gas that drives the three-dimensional rotating gliding arc plasma exciter comes from the inlet gas of the combustor. The swirling flow is generated by a vane-type axial flow swirled at the head without the use of external bleed air.

5.3. PAI/PAC high-fidelity multiphysics supplementary simulation model

Due to the low maturity of the current PAI/PAC technology, designers are mainly concentrated on the development of exciters and the mechanism of combustion [146–150]. The high experimental cost and limitations of detection methods have largely restricted the progress of experimental research. Therefore, numerical simulation of PAI/PAC in engine combustor is gradually becoming a research hotspot [151–156].

Plasma combustion has spanned multiple time and space scales; therefore, it is necessary to promote the PAI/PAC numerical simulation research with the advancement in multiphysics modeling and simulation. The simulation research of plasma enhanced combustion mainly includes the numerical simulation of the plasma excitation process and enhanced combustion process. The plasma-enhanced combustion process involves the combination of plasma dynamics and combustion dynamics. It is a typical multi-scale problem in space and time with large degrees of freedom, in which there is a strong coupling between electron and electromagnetic field. Because the associated physical and chemical processes are very complex, there are rigorous requirements on the mesh quality, discrete format, and solution method. Plasma enhanced combustion multiphysics modeling requires that electronic field, heat transfer, and turbulence were simultaneously

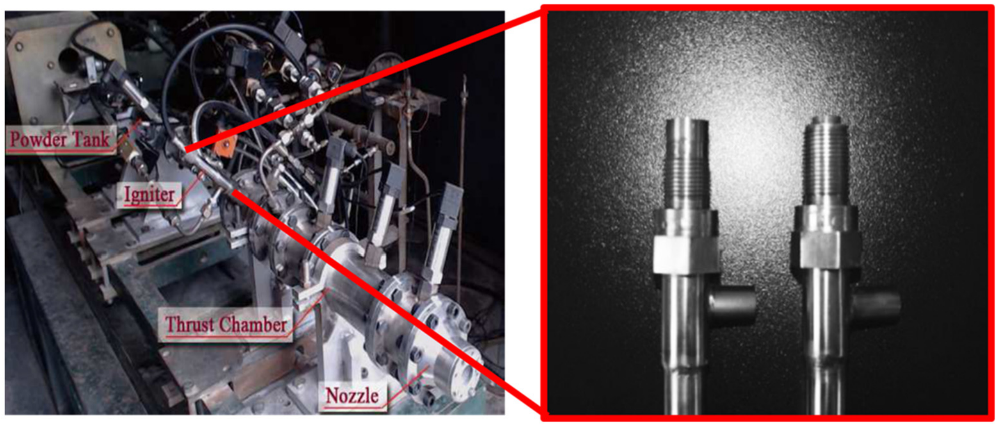

Fig. 33. A plasma igniter in the Mg/CO_2 powder engine. Reproduced from [135,136].

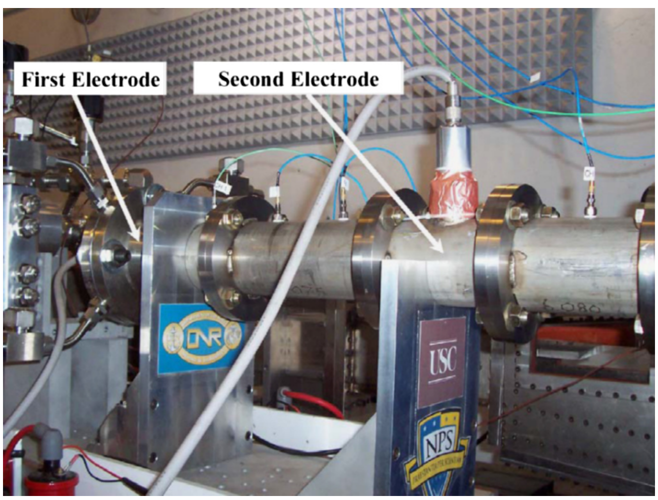

Fig. 34. Dual transient plasma ignition (TPI) electrode configuration. Reproduced from [139].

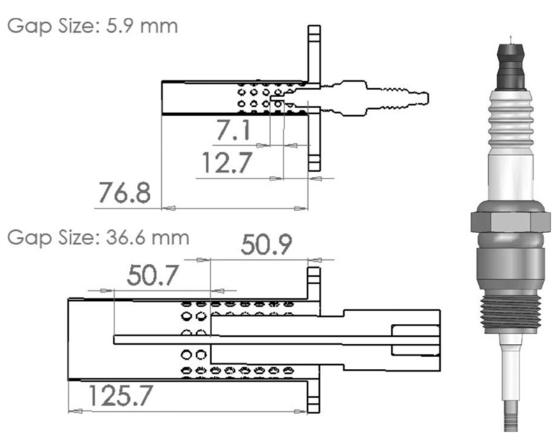

Fig. 35. A small plasma ignition device. Reproduced from [140].

coupled to simulate the fuel-air mixture, as described in Fig. 39 [56].

In current numerical simulations, the effects of plasma, which are represented by equivalent heating zone and active particle source term [47,72], generally enter the inlet boundary, fluid motion equation, and component transport equation without taking the plasma excitation process into account and establishing a multiphysics-field coupling model of plasma-enhanced combustion. The current DBD plasma actuation model established by com-

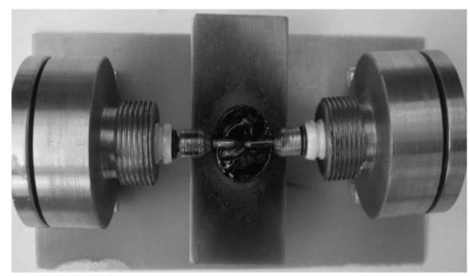

Fig. 36. Experimental device for plasma ignition of a paste propellant. Reproduced from [141].

mercial software has not been tested by experiments, and its accuracy is not guaranteed. The classical plasma model breaks down because the electrons move much faster than ions, the electron density in the sheath area is very low and the electric field strength is high. This is different from the study of plasma characteristics under simple conditions such as low pressure and static environment; the environmental conditions for plasma excitation and control combustion are very complicated, and the parameters such as flow velocity and pressure vary widely. Only with the help of high time-space resolution tests such as laser diagnosis and high accuracy modeling and simulation can we obtain key parameters such as electron density, electron temperature, reduced electric field, molecules in excited states, intermediate products, and the density of active radicals, etc. [157]. The specific type of plasma device depends on the application, and the physics governing the interaction between the plasma and the combustion processes, which can be drastically different from each other. A simple Venn diagram can illustrate the various interactions between plasma and combustion, as shown in Fig. 40 [158].

The simulation developed currently is generally for gaseous fuel. The composition of kerosene liquid combustion in the aerospace combustors is complex and it also involves atomization, evaporation and other processes, which makes the simulation more difficult. About the gaseous fuel, a zero-dimensional plasma-combustion simulation model is developed to calculate the time evolution of species and temperature in the hybrid NSD and DC discharge [155,156]. The model integrates the plasma kinetics solver ZDPlasKin [159] and the chemical kinetics solver CHEMKIN using a time-splitting method. The electron energy distribution function (EEDF) and the rate coefficients of electron impact reactions are calculated by a Boltzmann equation solver (BOLSIG+) [160] incorporated into ZDPlasKin. The numerical results using the above model agreed well with the experimental results about the species concentration, as shown in Fig. 41, which can validate the plasma-combustion kinetic model and the numerical methods.

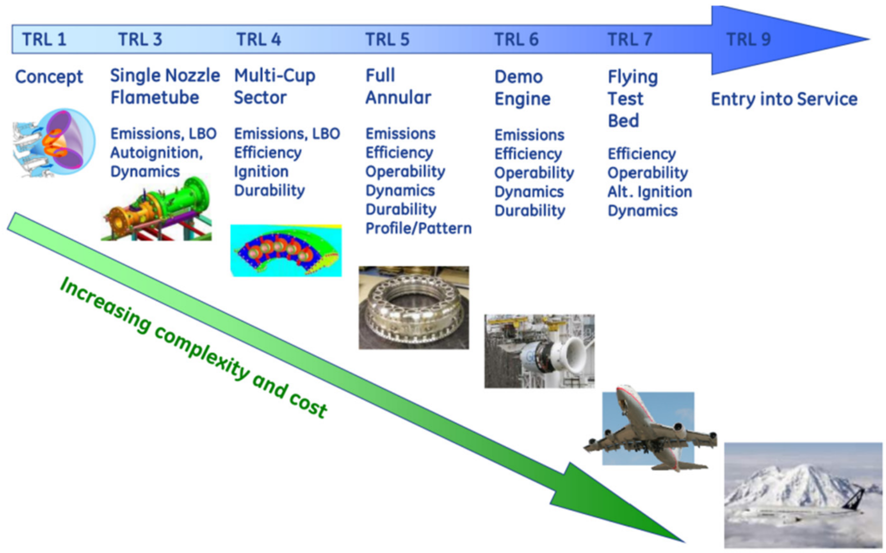

Fig. 37. Roadmap of the combustor technology development. Reproduced from [115].

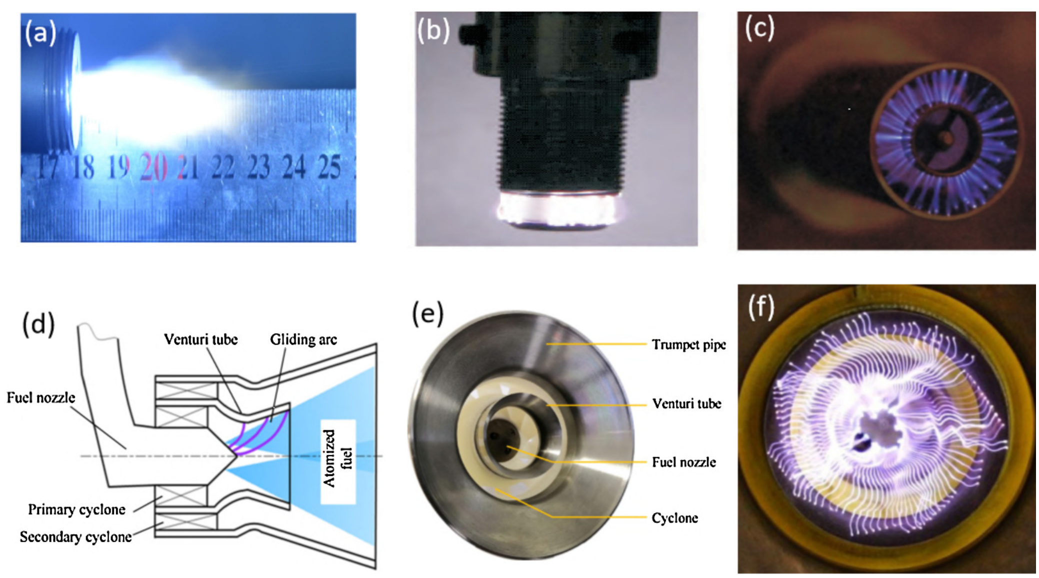

Fig. 38. Plasma igniter: (a) the plasma jet, (b) discharge photo of disc plasma igniter (nanosecond power), (c) toroidal plasma igniter. Discharge combustor head: (d) structure of the three-dimensional rotating gliding arc combustor, (e) structure of the combustor head, (f) discharge image of the combustor head. Reproduced from [38,144].

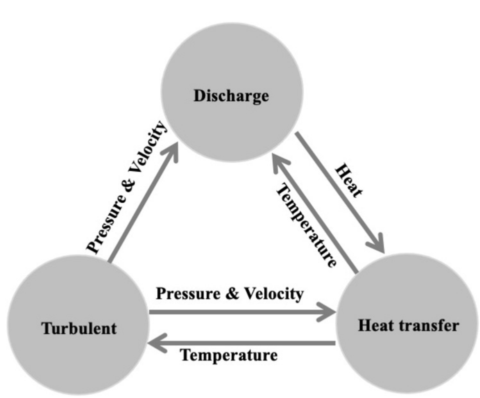

Fig. 39. Coupling of physics fields in plasma discharges simulation. Reproduced from [56].

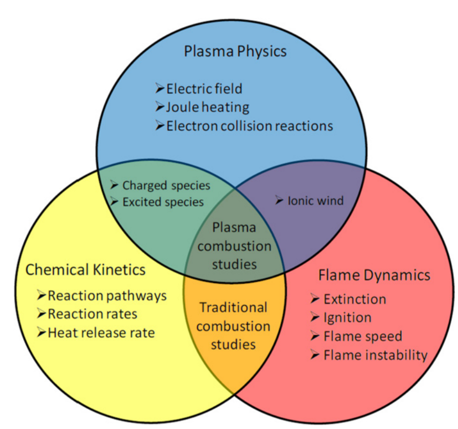

Fig. 40. Venn diagram of plasma and combustion interaction. Reproduced from [158].

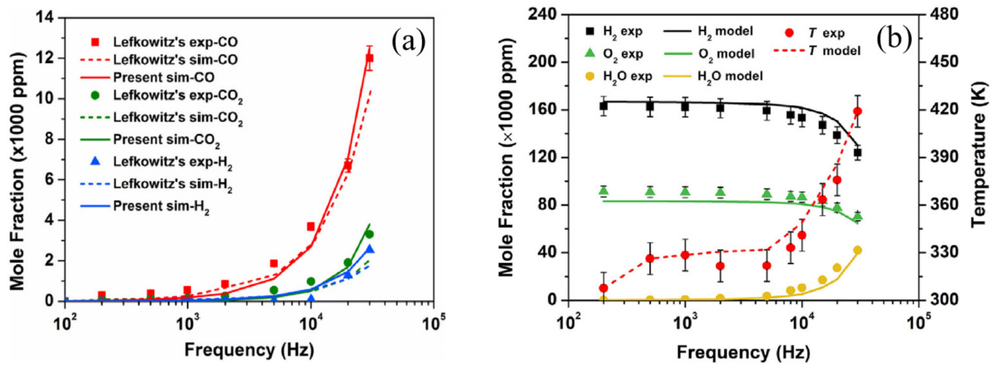

Fig. 41. (a) $CH_4/O_2/He$ mixtures, comparison of measured and predicted species in a continuous plasma up to 30 kHz repetition rate between the numerical model and Lefkowitz's [161] at 60 Torr. (b) $H_2/O_2/He$ mixtures, comparison of species concentration between steady state GC measurement and model prediction as well as measured temperature in a continuous nanosecond plasma ranging from 200 Hz to 30 kHz at 60 Torr. Dashed red line indicates the input temperature used in simulation. Reproduced from [155,156].

Specifically, BOLSIG+ is a Boltzmann equation solver. It provides information on collision cross sections according to electron energy. Thus, it is widely used in plasma kinetic modeling for many applications such as dielectric barrier discharge, nanosecond pulse discharge, and arc discharge. The main utility of BOLSIG+ is to obtain electron transport coefficients and collision rate coefficients from more fundamental cross section data, which can then be used as input for fluid models.

Future research needs to address the common requirements of PAI and PAC, establish a multiphysics coupling simulation model for plasma excitation, develop experimentally verified high-fidelity numerical simulation software, and provide guidance and tools for the performance optimization of PAI and PAC.

5.4. Artificial intelligence in the field of plasma ignition and combustion

Artificial Intelligence (abbreviated as AI) is a newly emerging science and technology that investigates and develops theories, methods, techniques and applications for simulating and expanding human intelligence. AI, as a wide-ranging branch of computer science, attempts to understand the essence of intelligence and build new smart machines capable of performing tasks that typically require human intelligence, i.e. they can react in a similar way to human intelligence. Research in this field includes robotics, language recognition, image recognition, natural language processing (NLP), and expert systems, etc. [162–165]. AI consists of five major branches, i.e. expert systems, artificial neural networks (ANNs), genetic algorithms (GA), fuzzy logic and various hybrid systems, which are combinations of two or more of the branches mentioned previously.

AI has gained rapid advancements in many technical fields including computer vision, speech recognition, machine learning, and natural language processing. New technical fields such as swarm intelligence, big data, and human-machine hybrid intelligence are becoming research hotspots in academia and industry. AI has penetrated into many areas ranging from medical care, security, to automobiles and robots, partially replacing the role of human beings. Also, the application of AI in the field of aerospace combustion attracts more and more attentions, as shown in Fig. 42. Artificial intelligence for the modeling and control of combustion processes is comprehensively reviewed [166]. It outlines an understanding of how AI systems operate by way of presenting a number of problems in the different disciplines of combustion engineering. Results presented in this paper, are testimony to the potential of AI as a design tool in many areas of combustion engineering. In the reference [167], artificial neural networks (ANN) technique combined with flamelet generated manifolds (FGM) is proposed to mitigate the memory issue of FGM models. It is shown that the present ANN models can properly replicate the FGM table for most of the species mass fractions. The network models with relative error less than 5% are considered in RANS and LES to simulate the Engine Combustion Network (ECN) Spray H flames. Also, Park predicted the operation characteristics of gas turbine combustor using ANN [168]. The predictive model was developed based on real-time operating data of gas turbine. It turns out that the model can be used for monitoring and diagnosing combustor operation.

Deep learning is a subset of a broader family of machine learning in AI that attempts to use multiple processing layers (neural networks) consisting of complex hierarchical structures or multiple nonlinear transformations to perform high-level abstract on data. Deep learning can be understood as the extension and development of neural networks. Neural networks are computing systems with interconnected nodes that work like neurons in the human brain and biological neural networks. Using algorithms, they can recognize hidden patterns and correlations in raw data, cluster and classify it, and continuously learn and improve in a similar manner to living things. Zhong et al. propose a deep learning method for solving the partial differential equations in thermal plasma models, as illustrated in Fig. 43 [169]. In this method a deep feedforward neural network is constructed to surrogate the solution of the model. They demonstrate the power of this deep learning method by solving a 1-D arc decaying model which consists of three cases: stationary arc, transient arc without considering radial velocity, and transient arc with radial velocity respectively. The results show that the deep neural networks have excellent ability to express the governing equations of thermal plasmas.

AI technology has brought about a new wave of applications in many fields such as autonomous driving, robotics, and medical treatment, the industry of aerospace engine should explore its possibilities. Considering the needs of industrial upgrading, AI has many potential applications in every part of the full life cycle of aerospace engine, and its perspective of application will also be broader. Therefore, in the future, AI will penetrate into the field of plasma ignition and combustion by providing a novel and powerful deep leaning technique to improve the numerical simulation method of solving plasma partial differential equations. Through AI and big data techniques, the data analysis and machine learning platform can be established to classify, regress and correlated the experimental data of plasma ignition and combustion, and extract their features, based on which a more realistic and comprehensive plasma combustion model can be developed. Such a model and its simulations can reduce the cost by partially replacing the expensive physical tests and also verify the previously developed plasma ignition and combustion models.

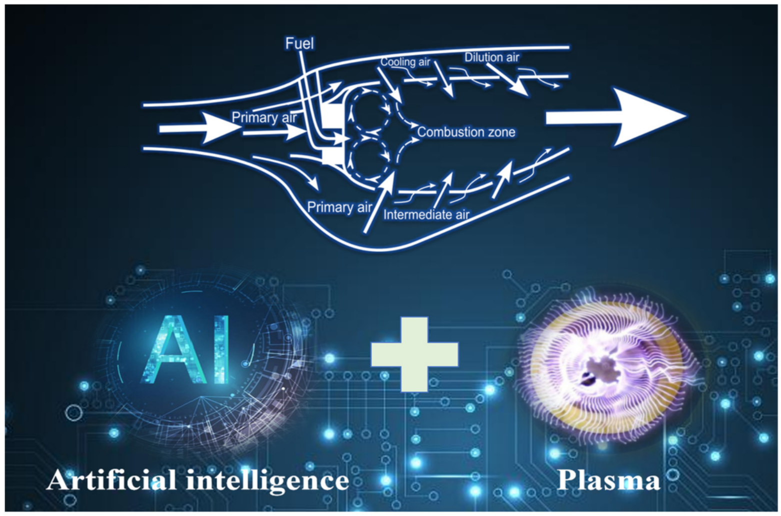

Fig. 42. Development perspective of combustor: AI combines with plasma ignition and combustion.

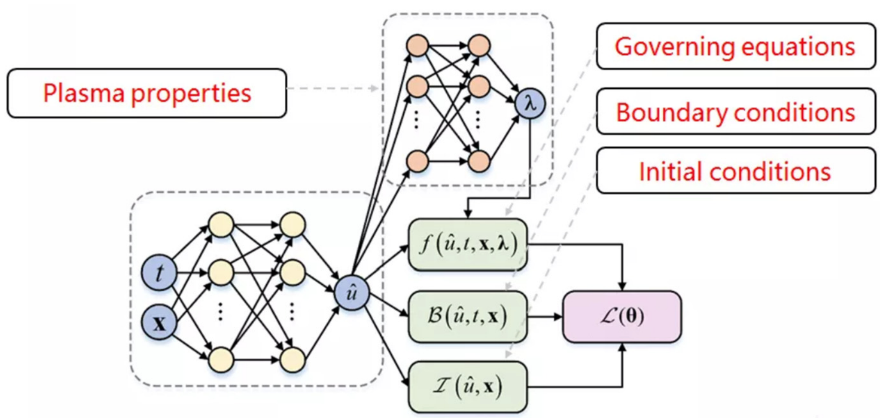

Fig. 43. Diagram of a deep neural network for thermal plasma modeling. A large multi-layer feed-forward neural network is used to surrogate the solution of differential equations describing thermal plasmas. A smaller neural network is used to express the plasma properties in differential equations. Reproduced from [169].

6. Concluding remarks

PAI has the following advantages. 1) The PAI source is a continuous high-temperature jet with a high energy of ignition and high efficiency for heating the unburned mixture; therefore, PAI is suitable for extreme environments. 2) The plasma igniter generates a high-speed jet and penetrates deep into the mixed gas. The plasma contacts the mixed gas inside the combustor liner and the ignition source can enter the central area of the combustor liner. PAI requires a low fuel-air ratio and airflow speed near the igniter. 3) The high-speed hot jet enhances the turbulent pulsation intensity of the airflow in the combustor and improves the mixing of fuel and air, facilitating the rapid atomization and evaporation of the fuel. 4) A large number of active atoms and groups generated during the discharge of PAI reduces the activation energy of the chemical reactions, shortens the ignition delay time, and accelerates the chemical kinetics of combustion.

Plasma technology has significant technical advantages for solving the key problems of combustion in advanced aerospace engines. PAI and PAC technology significantly improve the performance of the aero-engine combustors in high-altitude and extreme environments. Compared with electric spark ignition, PAI has higher spark energy and larger penetrating power, and directly ignites the atomized fuel. It challenges the traditional combustor through the head swirler (generating a recirculation zone to stabilize the flame). As Ref. [69] pointed out, Fig. 19 suggests that the improvement with NSPD is comparable if not better than the effect of increasing swirl number. This observation implies that the NSPD may completely augment or replace the role of swirl in the flame stabilization process. However, the complex coupling mechanism of the swirl flow and turbulent flame in the combustor of the swirl combustion mode remains a cosmopolitan science puzzle to date; at the same time, current PAI and PAC technology do not meet the requirements of engineering applications. The reasons are as follows. In order to improve the energy conversion efficiency and combustion enhancement effect of plasma excitation, it is needed to explore excitation methods with higher excitation intensity and higher efficiency on the basis of existing research. In order to have good compatibility with aircraft engines, it is necessary to develop plasma excitation equipment with small volume, small weight, long life, and suitable for a wide range of pressure, temperature, and humidity. The current manufacturing and processing of plasma igniter electrodes are quite difficult, and anode ablation is a big issue. It is urgent to explore more on the global design of the igniter and the selection and processing of electrode materials. Electromagnetic interference is relatively large in plasma excitation combustion, and electromagnetic pulse protection technology cannot meet the requirements [156]. Therefore, future research should be focused on two aspects: 1) clarify the mechanisms of swirling turbulent combustion, and 2) investigate the physical phenomena and internal mechanisms of PAI and PAC from multiple aspects. PAI and PAC technology show significant prospects for engineering applications since it provides reliable ignition and stable combustion of aerospace engines under extreme working environments.

Declaration of competing interest

The authors declare that they have no known competing financial interests or personal relationships that could have appeared to influence the work reported in this paper.

Acknowledgements

This work was supported by the National Natural Science Foundation of China (Grant Nos. 11972331 and 12072352), which is gratefully acknowledged by the authors.

References

[1] L. Rosocha, D. Coates, D. Platts, S. Stange, Plasma-enhanced combustion of propane using a silent discharge, Phys. Plasmas 11 (2004) 2950–2956.
[2] R. Weber, S. Orsino, N. Lallemant, A. Verlaan, Combustion of natural gas with high-temperature air and large quantities of flue gas, Proc. Combust. Inst. 28 (2000) 1315–1321.
[3] B. Gawron, T. Białecki, Impact of a Jet A-1/HEFA blend on the performance and emission characteristics of a miniature turbojet engine, Int. J. Environ. Sci. Technol. 15 (2018) 1501–1508.
[4] Z. Ren, B. Wang, G. Xiang, D. Zhao, L. Zheng, Supersonic spray combustion subject to scramjets: progress and challenges, Prog. Aerosp. Sci. 105 (2019) 40–59.
[5] C. Liu, M. Sun, H. Wang, L. Yang, B. An, Y. Pan, Ignition and flame stabilization characteristics in an ethylene-fueled scramjet combustor, Aerosp. Sci. Technol. 106 (2020) 106186.
[6] S. Huang, Z. Zhang, H. Song, Y. Wu, Y. Li, A novel way to enhance the spark plasma-assisted ignition for an aero-engine under low pressure, Appl. Sci. 8 (2018) 1533.
[7] A. Bellemans, N. Deak, F. Bisetti, Development of skeletal kinetics mechanisms for plasma-assisted combustion via principal component analysis, Plasma Sources Sci. Technol. 29 (2020) 025020.
[8] A. Rousso, X. Mao, Q. Chen, Y. Ju, Kinetic studies and mechanism development of plasma assisted pentane combustion, Proc. Combust. Inst. 37 (2019) 5595–5603.
[9] S. Wang, J. Yu, W. Cheng, Y. Ma, R. Zheng, D. Huang, Q. Wei, Chemical kinetic analysis of plasma excited methane combustion, Chem. Phys. Lett. 730 (2019) 399–406.
[10] X. Mao, Q. Chen, A.C. Rousso, T.Y. Chen, Y. Ju, Effects of controlled non-equilibrium excitation on $H_2/O_2/He$ ignition using a hybrid repetitive nanosecond and DC discharge, Combust. Flame 206 (2019) 522–535.
[11] A. Bourig, Combustion modification by non-thermal plasma, Dissertation, zur Erlangung des akademischen Grades, 2009.
[12] A.Y. Starikovskii, Plasma supported combustion, Proc. Combust. Inst. 30 (2005) 2405–2417.
[13] R. Goldston, P. Rutherford, Introduction to Plasma Physics, Taylor & Francis Group, 1995.
[14] N. Venkatramani, Industrial plasma torches and applications, Curr. Sci. (2002) 254–262.
[15] I. Adamovich, I. Choi, N. Jiang, J. Kim, S. Keshav, W. Lempert, E. Mintusov, M. Nishihara, M. Samimy, M. Uddi, Plasma assisted ignition and high-speed flow control: non-thermal and thermal effects, Plasma Sources Sci. Technol. 18 (2009) 034018.
[16] Z. Chen, G. Li, Z. Wu, Y. Xia, The crack propagating behavior of composite coatings prepared by PEO on aluminized steel during in situ tensile processing, Mater. Sci. Eng. A 528 (2011) 1409–1414.
[17] C.R. Vandenabeele, S. Lucas, Technological challenges and progress in nanomaterials plasma surface modification–a review, Mater. Sci. Eng., R Rep. 139 (2020) 100521.
[18] G. Chen, Z. Chen, D. Wen, Z. Wang, H. Li, Y. Zeng, G. Dotti, R.E. Wirz, Z. Gu, Transdermal cold atmospheric plasma-mediated immune checkpoint blockade therapy, Proc. Natl. Acad. Sci. 117 (2020) 3687–3692.
[19] Z. Chen, G. Peng, P. Chen, Y. Xia, G. Li, Investigation of the tribological behavior of chromium aluminum silicon nitride coatings via both scratch sliding test and FEM simulation, AIP Adv. 9 (2019) 025116.
[20] P.K. Chu, Applications of plasma-based technology to microelectronics and biomedical engineering, Surf. Coat. Technol. 203 (2009) 2793–2798.
[21] Z. Chen, H. Simonyan, X. Cheng, E. Gjika, L. Lin, J. Canady, J.H. Sherman, C. Young, M. Keidar, A novel micro cold atmospheric plasma device for glioblastoma both in vitro and in vivo, Cancers 9 (2017) 61.
[22] Z. Chen, S. Zhang, I. Levchenko, I.I. Beilis, M. Keidar, In vitro demonstration of cancer inhibiting properties from stratified self-organized plasma-liquid interface, Sci. Rep. 7 (2017) 12163.
[23] W. Li, H. Yu, D. Ding, Z. Chen, Y. Wang, S. Wang, X. Li, M. Keidar, W. Zhang, Cold atmospheric plasma and iron oxide-based magnetic nanoparticles for synergetic lung cancer therapy, Free Radic. Biol. Med. 130 (2019) 71–81.
[24] Z. Chen, R.-G. Xu, P. Chen, Q. Wang, Potential agricultural and biomedical applications of cold atmospheric plasma-activated liquids with self-organized patterns formed at the interface, IEEE Trans. Plasma Sci. 48 (2020) 3455–3471.
[25] Z. Chen, G. Garcia Jr, V. Arumugaswami, R.E. Wirz, Cold atmospheric plasma for SARS-CoV-2 inactivation, Phys. Fluids 32 (2020) 111702.
[26] S.M. Starikovskaia, Plasma assisted ignition and combustion, J. Phys. D, Appl. Phys. 39 (2006) R265.
[27] Y. Ju, W. Sun, Plasma assisted combustion: dynamics and chemistry, Prog. Energy Combust. Sci. 48 (2015) 21–83.
[28] W. Sun, Non-Equilibrium Plasma-Assisted Combustion, Princeton University, 2013.
[29] L. He, X. Liu, B. Zhao, Current investigation progress of plasma-assisted ignition and combustion, J. Aerosp. Power 31 (2016) 1537–1551.
[30] L. He, W. Qi, B. Zhao, G. Chen, X. Bai, K. Duan, Analysis of the dynamic process of air plasma jet, High Volt. Eng. 41 (2015) 2030–2036.
[31] Y. Lan, L. He, W. Ding, Investigation and simulation of dielectric barrier discharge under high frequency and high voltage, High Volt. Apparatus 46 (2010) 35–38.
[32] R. Snoeckx, M.S. Cha, Inevitable chemical effect of balance gas in low temperature plasma assisted combustion, Combust. Flame 225 (2020) 1–4.
[33] J. Warnatz, U. Maas, R.W. Dibble, Physical and Chemical Fundamentals, Modeling and Simulation, Experiments, Pollutant Formation, Springer, 1990.
[34] P. Song, L. Chen, C. Gong, The progress in non-equilibrium plasma assistant ignition of gaseous fuel, J. Dalian Minzu Univ. 18 (2016) 38–42.
[35] W. Roquemore, D. Shouse, D. Burrus, A. Johnson, C. Cooper, B. Duncan, K.-Y. Hsu, V. Katta, G. Sturgess, I. Vihinen, Vortex combustor concept for gas turbine engines, in: 39th Aerospace Sciences Meeting and Exhibit, 2001, p. 483.
[36] S. Blakey, L. Rye, C.W. Wilson, Aviation gas turbine alternative fuels: a review, Proc. Combust. Inst. 33 (2011) 2863–2885.
[37] M. Dong, J. Cui, M. Jia, Y. Shang, S. Li, Large eddy simulation of plasma-assisted ignition and combustion in a coaxial jet combustor, Energy (2020) 117463.
[38] B.-b. Zhao, G.-C. Chen, L.-M. He, T. Jin, B. Jing, Experimental investigation of plasma jet ignition characteristics in kerosene–air mixtures, J. Aerosp. Eng. 33 (2020) 04019113.
[39] R. Feng, J. Li, Y. Wu, M. Jia, D. Jin, Ignition and blow-off process assisted by the rotating gliding arc plasma in a swirl combustor, Aerosp. Sci. Technol. 99 (2020) 105752.
[40] S. Zare, H.W. Lo, S. Roy, O. Askari, On the low-temperature plasma discharge in methane/air diffusion flames, Energy 197 (2020) 117185.
[41] H. Zheng, Z. Zhihao, L. Xiao, Study on plasma ignition characteristics of micro gas turbine combustor burning low calorific value fuel, J. Harbin Eng. Univ. 6 (2020) 1–8.
[42] G.T. Kim, C.S. Yoo, S.H. Chung, J. Park, Effects of non-thermal plasma on the lean blowout limits and CO/NO_x emissions in swirl-stabilized turbulent lean-premixed flames of methane/air, Combust. Flame 212 (2020) 403–414.
[43] C. Guo, Research on plasma assisted suppression of combustion oscillation, PhD Dissertation, Harbin Institute of Technology, China, 2019.
[44] Z. Wei, Study on low temperature plasma assisted combustion under high pressure, Dissertation, Shengyang Aerospace University, China, 2019.
[45] Y. Chen, L. Fei, L. He, L. Zhang, C. Zhu, J. Deng, The influence of dielectric barrier discharge plasma on the characteristics of aero-engine combustion chamber, Xibei Gongye Daxue Xuebao/J. Northwest. Polytech. University 37 (2019) 369–377.
[46] Z. Zhao, L. He, H. Zhang, et al., Effect of swirler chamfer angle in air plasma igniter on characteristics of igniter, High Volt. Eng. 45 (2019) 1921–1928, https://doi.org/10.13336/j.1003-6520.hve.20181205003.
[47] F. Li, L. He, Y. Chen, Numerical study on plasma-assisted combustion in one type of aero-engine combustion chamber, J. Combust. Sci. Technol. 25 (2019) 451–459.
[48] W. Kim, J. Cohen, Plasma-assisted combustor dynamics control at realistic gas turbine conditions, Combust. Sci. Technol. (2019) 1–20.
[49] J. Deng, C. Peng, L. He, S. Wang, J. Yu, B. Zhao, Effects of dielectric barrier discharge plasma on the combustion performances of reverse-flow combustor in an aero-engine, J. Therm. Sci. 28 (2019) 1035–1041.
[50] X. Liu, L. He, C. Yi, J. Lei, J. Deng, Emission characteristics of aviation kerosene combustion in aero-engine annular combustor with low temperature plasma assistance, Therm. Sci. 23 (2019) 647–660.
[51] S. Liu, N. Zhao, J. Zhang, J. Yang, Z. Li, H. Zheng, Experimental and numerical investigations of plasma ignition characteristics in gas turbine combustors, Energies 12 (2019) 1511.
[52] B. Lin, Y. Wu, Y. Zhu, F. Song, D. Bian, Experimental investigation of gliding arc plasma fuel injector for ignition and extinction performance improvement, Appl. Energy 235 (2019) 1017–1026.
[53] L. He, Y. Chen, J. Deng, J. Lei, F. Li, P. Liu, Experimental study of rotating gliding arc discharge plasma-assisted combustion in an aero-engine combustion chamber, Chin. J. Aeronaut. 32 (2019) 337–346.

[54] A. Mardani, A. Khanehzar, Numerical assessment of MILD combustion enhancement through plasma actuator, Energy 183 (2019) 172–184.
[55] S. Song, L. Kong, J. Yang, Numerical simulation and experimental study on plasma ignition and combustion enhancement, Gas Turbine Technol. 2 (2019) 34–39.
[56] D. Jun, H. Liming, L. Xingjian, C. Yi, Numerical simulation of plasma-assisted combustion of methane-air mixtures in combustion chamber, Plasma Sci. Technol. 20 (2018) 125502.
[57] H.-L. Zhang, L.-M. He, G.-C. Chen, W.-T. Qi, J.-L. Yu, Experimental study on ignition characteristics of kerosene–air mixtures in V-shaped burner with DC plasma jet igniter, Aerosp. Sci. Technol. 74 (2018) 56–62.
[58] H. Zhang, H. Liming, Y. Jinlu, Q. Wentao, C. Gaocheng, Investigation of flame structure in plasma-assisted turbulent premixed methane-air flame, Plasma Sci. Technol. 20 (2018) 024001.
[59] W. Dai, L. He, H. Zhang, Experimental investigation for effects of anode channel length on characteristics of plasma jet igniter, J. Propuls. Technol. 39 (2018) 1568–1575.
[60] X. Zhan, C. Jian, Y. Ting, J. Rongwei, Experimental investigation of plasma ignition in an annular reverse-flow combustor, Gas Turbine Exp. Res. 31 (2018) 37–40.
[61] F. Gomez del Campo, D.E. Weibel, C. Wen, Preliminary results from a plasma-assisted 7-point Lean Direct Injection (LDI) combustor and resulting impacts on combustor stability and combustion dynamics, in: 53rd AIAA/SAE/ASEE Joint Propulsion Conference, 2017, p. 4778.
[62] G.T. Kim, B.H. Seo, W.J. Lee, J. Park, M.K. Kim, S.M. Lee, Effects of applying non-thermal plasma on combustion stability and emissions of NO_x and CO in a model gas turbine combustor, Fuel 194 (2017) 321–328.
[63] X. Liu, L. He, Y. Tao, Investigation of effects of plasma-assisted combustion on lean-fuel combustion of aviation kerosene, J. Propuls. Technol. 37 (2016) 1727–1734.
[64] W. Qi, L. He, Z. Bingbing, Experimental investigation on air plasma jet igniter characteristics, J. Propuls. Technol. 37 (2016) 2107–2113.
[65] J. Sagás, H. Maciel, P. Lacava, Effects of non-steady state discharge plasma on natural gas combustion: flammability limits, flame behavior and hydrogen production, Fuel 182 (2016) 118–123.
[66] R. Rajasegar, C.M. Mitsingas, E.K. Mayhew, J. Yoo, T. Lee, Proper orthogonal decomposition for analysis of plasma-assisted premixed swirl-stabilized flame dynamics, IEEE Trans. Plasma Sci. 44 (2016) 2940–2951.
[67] R. Rajasegar, C.M. Mitsingas, E.K. Mayhew, S. Hammack, H. Do, T. Lee, Effects of continuous volumetric direct-coupled nonequilibrium atmospheric microwave plasma discharge on swirl-stabilized premixed flames, IEEE Trans. Plasma Sci. 44 (2016) 39–48.
[68] S. Barbosa, G. Pilla, D. Lacoste, P. Scouflaire, S. Ducruix, C.O. Laux, D. Veynante, Influence of nanosecond repetitively pulsed discharges on the stability of a swirled propane/air burner representative of an aeronautical combustor, Philos. Trans. R. Soc., Math. Phys. Eng. Sci. 373 (2015) 20140335.
[69] W. Kim, J. Snyder, J. Cohen, Plasma assisted combustor dynamics control, Proc. Combust. Inst. 35 (2015) 3479–3486.
[70] A. Ehn, J. Zhu, P. Petersson, Z. Li, M. Aldén, C. Fureby, T. Hurtig, N. Zettervall, A. Larsson, J. Larfeldt, Plasma assisted combustion: effects of O_3 on large scale turbulent combustion studied with laser diagnostics and large eddy simulations, Proc. Combust. Inst. 35 (2015) 3487–3495.
[71] M.G. De Giorgi, A. Sciolti, S. Campilongo, E. Pescini, A. Ficarella, L.M. Martini, P. Tosi, G. Dilecce, Plasma assisted flame stabilization in a non-premixed lean burner, Energy Proc. 82 (2015) 410–416.
[72] X. Liu, L. He, S. Zhenxing, Numerical simulation of plasma assisted combustion and traditional combustion in combustion chamber, J. Combust. Sci. Technol. 21 (2015) 135–140.
[73] S. Nagaraja, V. Yang, Z. Yin, I. Adamovich, Ignition of hydrogen–air mixtures using pulsed nanosecond dielectric barrier plasma discharges in plane-to-plane geometry, Combust. Flame 161 (2014) 1026–1037.
[74] B. Zhao, L. He, Y. Lan, W. Ding, Y. Wang, Experimental investigation of igniting characteristics of plasma jet igniter, High Volt. Eng. 7 (2013) 1687–1697.
[75] J. Moeck, D. Lacoste, C. Laux, C. Paschereit, Control of combustion dynamics in a swirl-stabilized combustor with nanosecond repetitively pulsed discharges, in: 51st AIAA Aerospace Sciences Meeting Including the New Horizons Forum and Aerospace Exposition, 2013, p. 565.
[76] D. Lacoste, D. Xu, J. Moeck, C. Laux, Dynamic response of a weakly turbulent lean-premixed flame to nanosecond repetitively pulsed discharges, Proc. Combust. Inst. 34 (2013) 3259–3266.
[77] D.A. Lacoste, J.P. Moeck, C.O. Paschereit, C.O. Laux, Effect of plasma discharges on nitric oxide emissions in a premixed flame, J. Propuls. Power 29 (2013) 748–751.
[78] D.H. Lee, K.-T. Kim, H.S. Kang, Y.-H. Song, J.E. Park, Plasma-assisted combustion technology for NO_x reduction in industrial burners, Environ. Sci. Technol. 47 (2013) 10964–10970.
[79] Z. Song, L. He, J. Su, B. Zhao, Y. Lan, X. Liu, Numerical simulation of inlet parameters influence on plasma ignition process, High Volt. Eng. 39 (2013) 903–910.
[80] Z. Yin, A. Montello, C.D. Carter, W.R. Lempert, I.V. Adamovich, Measurements of temperature and hydroxyl radical generation/decay in lean fuel–air mixtures excited by a repetitively pulsed nanosecond discharge, Combust. Flame 160 (2013) 1594–1608.
[81] Z. Yin, I. Adamovich, W. Lempert, OH radical and temperature measurements during ignition of h_2-air mixtures excited by a repetitively pulsed nanosecond discharge, Proc. Combust. Inst. 34 (2013) 3249–3258.
[82] D.H. Lee, K.-T. Kim, H.S. Kang, Y.-H. Song, J.E. Park, NO_x reduction strategy by staged combustion with plasma-assisted flame stabilization, Energy Fuels 26 (2012) 4284–4290.
[83] B.-B. Zhao, P. Zhang, L.-M. He, H.-L. Du, Experiments of plasma assisted combustion's effect on combustion products, J. Aerosp. Power 27 (2012) 1974–1978.
[84] I. Choi, Z. Yin, I.V. Adamovich, W.R. Lempert, Hydroxyl radical kinetics in repetitively pulsed hydrogen–air nanosecond plasmas, IEEE Trans. Plasma Sci. 39 (2011) 3288–3299.
[85] S. Serbin, A. Mostipanenko, I. Matveev, A. Topina, Improvement of the gas turbine plasma assisted combustor characteristics, in: 49th AIAA Aerospace Sciences Meeting Including the New Horizons Forum and Aerospace Exposition, 2011, p. 61.
[86] J.D. Dale, M. Checkel, P. Smy, Application of high energy ignition systems to engines, Prog. Energy Combust. Sci. 23 (1997) 379–398.
[87] A.H. Lefebvre, Gas Turbine Combustion, CRC Press, 1998.
[88] N. Kawahara, S. Hashimoto, E. Tomita, Spark discharge ignition process in a spark-ignition engine using a time series of spectra measurements, Proc. Combust. Inst. 36 (2017) 3451–3458.
[89] K. Prieur, D. Durox, J. Beaunier, T. Schuller, S. Candel, Ignition dynamics in an annular combustor for liquid spray and premixed gaseous injection, Proc. Combust. Inst. 36 (2017) 3717–3724.
[90] B.-H. Cai, H.-M. Song, M. Jia, Y. Wu, W. Cui, S.-F. Huang, Experimental study on energy characteristics and ignition performance of recessed multichannel plasma igniter, Chin. Phys. B 29 (2020) 065207.
[91] Yoshinori Matsubara, Kenichi Takita, Goro Masuya, Combustion enhancement in a supersonic flow by simultaneous operation of DBD and plasma jet, Proc. Combust. Inst. 34 (2013) 3287–3294.
[92] I.N. Kosarev, S.V. Kindysheva, R.M. Momot, E.A. Plastinin, N.L. Aleksandrov, A.Yu. Starikovskiy, Comparative study of nonequilibrium plasma generation and plasma-assisted ignition for C_2-hydrocarbons, Combust. Flame 165 (2016) 259–271.
[93] M.P. Bulat, P.V. Bulat, P.V. Denissenko, I.I. Esakov, L.P. Grachev, P.V. Lavrov, K.N. Volkov, I.A. Volobuev, Plasma-assisted ignition and combustion of lean and rich air/fuel mixtures in low- and high-speed flows, Acta Astronaut. 176 (2020) 700–709.
[94] Hyungrok Do, Mark A. Cappelli, M. Godfrey Mungal, Plasma assisted cavity flame ignition in supersonic flows, Combust. Flame 157 (2010) 1783–1794.
[95] M. Stöhr, I. Boxx, C. Carter, W. Meier, Dynamics of lean blowout of a swirl-stabilized flame in a gas turbine model combustor, Proc. Combust. Inst. 33 (2011) 2953–2960.
[96] N. Chintala, A. Bao, G. Lou, I.V. Adamovich, Measurements of combustion efficiency in nonequilibrium RF plasma-ignited flows, Combust. Flame 144 (2006) 744–756.
[97] G. Li, X. Jiang, Z. Lei, et al., Central recirculation zone induced by the DBD plasma actuation, Sci. Rep. 10 (2020) 13004.
[98] Kavindu Ranasinghe, Kai Guan, Alessandro Gardi, Roberto Sabatini, Review of advanced low-emission technologies for sustainable aviation, Energy 188 (2019) 115945.
[99] A. Prakash, Prediction of NO_x emissions for an RQL aero-engine combustor using a stirred reactor modelling approach, in: 52nd AIAA/SAE/ASEE Joint Propulsion Conference, 25–27 July 2016, 2016, pp. 25–27.
[100] S.K. Dhanuka, J.E. Temme, J.F. Driscoll, Unsteady aspects of lean premixed prevaporized gas turbine combustors: flame-flame interactions, J. Propuls. Power 27 (2011) 631–641.
[101] C.-M. Lee, K. Chun, R. Locke, Fuel-air mixing effect on NO_x emissions for a lean premixed-prevaporized combustion system, in: 33rd Aerospace Sciences Meeting and Exhibit, 1995, p. 729.
[102] K.-S. Im, S. Subramaniyam, A. Mulemane, M.-C. Lai, Spray and fuel-air mixing of the swirler/venturi injectors for lean premixed prevaporized combustor, in: 42nd AIAA Aerospace Sciences Meeting and Exhibit, 2001, pp. 134.
[103] A. Dasgupta, Z. Li, T. Shih, K. Kundu, J. Deur, Computations of spray, fuel-air mixing, and combustion in a lean-premixed-prevaporized combustor, in: 29th Joint Propulsion Conference and Exhibit, 1993, p. 2069.
[104] C.M. Heath, Characterization of swirl-venturi lean direct injection designs for aviation gas turbine combustion, J. Propuls. Power 30 (2014) 1334–1356.
[105] K.M. Tacina, C. Chang, Z.J. He, P. Lee, H.C. Mongia, B.K. Dam, A second generation swirl-venturi lean direct injection combustion concept, in: 50th AIAA/ASME/SAE/ASEE Joint Propulsion Conference, 2014, p. 3434.
[106] R.R. Tacina, P. Lee, C. Wey, A lean-direct-injection combustor using a 9 point swirl-venturi fuel injector, ISABE 2005-1106, 2005.
[107] K. Ajmani, P. Lee, C.T. Chang, M.T. Kudlac, CFD evaluation of lean-direct injection combustors for commercial supersonics technology, in: AIAA Propulsion and Energy 2019 Forum, 2019, p. 4199.

[108] W.A. Acosta, C. Chang, Experimental combustion dynamics behavior of a multi-element Lean Direct Injection (LDI) gas turbine combustor, in: 52nd AIAA/SAE/ASEE Joint Propulsion Conference, 2016, p. 4589.
[109] Jianzhong Li, Jian Chen, Wu Jin, Li Yuan, Ge Hu, The design and performance of a RP-3 fueled high temperature rise combustor based on RQL staged combustion, Energy 209 (2020) 118480.
[110] O.C. Kocaman, T. Aksu, S. Uslu, Large-eddy simulation of a full annular RQL combustion chamber & fuel distribution effects on the combustor exit temperature profile, in: 52nd AIAA/SAE/ASEE Joint Propulsion Conference, 2016, p. 4786.
[111] I. El Helou, A. Skiba, E. Mastorakos, J.A. Sidey, Investigation of the effect of dilution air on soot production and oxidation in a lab scale Rich-Quench-Lean (RQL) burner, in: AIAA Scitech 2019 Forum, 2019, p. 1436.
[112] R. McKinney, A. Cheung, W. Sowa, D. Sepulveda, The Pratt & Whitney TALON X low emissions combustor: revolutionary results with evolutionary technology, in: 45th AIAA Aerospace Sciences Meeting and Exhibit, 2007, p. 386.
[113] Jian Chen, Jianzhong Li, Li Yuan, Ge Hu, Flow and flame characteristics of a RP-3 fuelled high temperature rise combustor based on RQL, Fuel 235 (2019) 1159–1171.
[114] H. Mongia, TAPS: a fourth generation propulsion combustor technology for low emissions, in: AIAA International Air and Space Symposium and Exposition: the Next 100 Years, 2003, p. 2657.
[115] M. Foust, D. Thomsen, R. Stickles, C. Cooper, W. Dodds, Development of the GE aviation low emissions TAPS combustor for next generation aircraft engines, in: 50th AIAA Aerospace Sciences Meeting Including the New Horizons Forum and Aerospace Exposition, 2012, p. 936.
[116] Y.R. Hicks, T. Capil, R. Anderson, Flame tube testing of a GEA TAPS injector: effects of fuel staging on combustor fuel spray patterns, flow structure, and speciation, in: 2018 Joint Propulsion Conference, 2018, p. 4476.
[117] K.-Y. Hsu, L. Goss, W. Roquemore, Characteristics of a trapped-vortex combustor, J. Propuls. Power 14 (1998) 57–65.
[118] Z. Jingyu, H. Xiaomin, W. Lu, J. Yi, Experimental and numerical investigations on liner cooling characteristics of a trapped vortex combustor, Appl. Therm. Eng. 80 (2015) 66–75.
[119] Zhikai Wang, Zhuoxiong Zeng, Kai Li, Yihua Xu, Effect of structure parameters of the flow guide vane on cold flow characteristics in trapped vortex combustor, J. Hydrodyn. 27 (2015) 730–737.
[120] D. Zhao, E. Gutmark, P. de Goey, A review of cavity-based trapped vortex, ultra-compact, high-g, inter-turbine combustors, Prog. Energy Combust. Sci. 66 (2018) 42–82.
[121] P. Jiang, X. He, Performance of a novel mixed-flow trapped vortex combustor for turboshaft engine, Aerosp. Sci. Technol. 105 (2020) 106034.
[122] Y. Zhao, X. He, J. Xiao, M. Li, Effect of cavity-air injection mode on the performance of a trapped vortex combustor, Aerosp. Sci. Technol. 106 (2020) 106183.
[123] Z. Wang, Z. Zeng, X. Yihua, Numerical simulation of open structure of rear blunt body in advanced vortex combustor, J. Propuls. Technol. 35 (2014) 809–814.
[124] Z. Wang, Z. Zeng, X. Yihua, Effects of flow guide vanes structure parameters on characteristics of advanced vortex combustor, J. Propuls. Technol. 36 (2015) 405–412.
[125] Zhuoxiong Zeng, Haoyuan Wang, Zhikai Wang, Analysis of cooling performance and combustion flow in advanced vortex combustor with guide vane, Aerosp. Sci. Technol. 72 (2018) 542–552.
[126] Haijun Sun, Pinghua Yan, Yihua Xu, Numerical simulation on hydrogen combustion and flow characteristics of a jet-stabilized combustor, Int. J. Hydrog. Energy 45 (2020) 12604–12615.
[127] Guoyu Ding, Xiaomin He, Ziqiang Zhao, Bokun An, Yaoyu Song, Yixiao Zhu, Effect of dilution holes on the performance of a triple swirler combustor, Chin. J. Aeronaut. 27 (2014) 1421–1429.
[128] K. McManus, T. Poinsot, S.M. Candel, A review of active control of combustion instabilities, Prog. Energy Combust. Sci. 19 (1993) 1–29.
[129] Aurélie Bellemans, Nicholas Kincaid, Nicholas Deak, Perrine Pepiot, Fabrizio Bisetti, P-DRGEP: a novel methodology for the reduction of kinetics mechanisms for plasma-assisted combustion applications, Proc. Combust. Inst. (2020), https://doi.org/10.1016/j.proci.2020.06.363.
[130] A. Starikovskiy, Physics and Chemistry of Plasma-Assisted Combustion, The Royal Society Publishing, 2015.
[131] Rajesh Kumar Prasad, Avinash Kumar Agarwal, Development and comparative experimental investigations of laser plasma and spark plasma ignited hydrogen enriched compressed natural gas fueled engine, Energy 216 (2021) 119282.
[132] Chao Li, Chunbo Hu, Zhe Deng, Xu Hu, Yue Li, Jinjia Wei, Dynamic ignition and combustion characteristics of agglomerated boron-magnesium particles in hot gas flow, Aerosp. Sci. Technol. 110 (2021) 106478.
[133] J. Yuan, J. Liu, Y. Zhou, Y. Zhang, K. Cen, Thermal decomposition and combustion characteristics of Al/AP/HTPB propellant, J. Therm. Anal. Calorim. (2020) 1–10.
[134] C. Li, C. Hu, X. Zhu, J. Hu, Y. Li, X. Hu, Experimental study on the thrust modulation performance of powdered magnesium and CO_2 bipropellant engine, Acta Astronaut. 147 (2018) 403–411.
[135] Y. Li, C. Hu, X. Zhu, J. Hu, X. Hu, C. Li, Y. Cai, Experimental study on combustion characteristics of powder magnesium and carbon dioxide in rocket engine, Acta Astronaut. 155 (2019) 334–349.
[136] C. Hu, C. Li, Z. Deng, Principle of Powder Rocket Engine, National Defense Industry Press, China, 2019.
[137] James T. Peace, Frank K. Lu, Performance modeling of pulse detonation engines using the method of characteristics, Aerosp. Sci. Technol. 88 (2019) 51–64.
[138] F. Wang, C. Jiang, A. Kuthi, M. Gundersen, J. Sinibaldi, C. Brophy, L. Lee, Transient plasma ignition of hydrocarbon-air mixtures in pulse detonation engines, in: 42nd AIAA Aerospace Sciences Meeting and Exhibit, 2004, p. 834.
[139] J. Sinibaldi, J. Rodriguez, B. Channel, C. Brophy, F. Wang, C. Cathey, M. Gundersen, Investigation of transient plasma ignition for pulse detonation engines, in: 41st AIAA/ASME/SAE/ASEE Joint Propulsion Conference & Exhibit, 2005, p. 3774.
[140] D.R. Singleton, J.O. Sinibaldi, C.M. Brophy, A. Kuthi, M.A. Gundersen, Compact pulsed-power system for transient plasma ignition, IEEE Trans. Plasma Sci. 37 (2009) 2275–2279.
[141] S. Zhou, Y. Zheng, Y. Ju, Research on application of composite plasma igniting pasty propellant, J. Ballist. (2008).
[142] S.-g. Zhou, Y. Zheng, Y.-t. Ju, C. Zhou, J.-x. Zhou, Realization and simulation of rocket multiple ignition system based on fuzzy control air-pasty, in: 2008 Asia Simulation Conference-7th International Conference on System Simulation and Scientific Computing, IEEE, 2008, pp. 1147–1150.
[143] S. Zhou, The study on multiple starts of pasty propellant rocket, Dissertation, Nanjing University of Science and Technology, 2009.
[144] Z. Chen, J. Yu, L. Zhang, l. Jiang, Y. Jiang, Y. Hu, Experimental study on working characteristics of new combustion chamber head based on plasma, J. Propuls. Technol. 41 (2020) 2766–2773.
[145] X. Rao, S. Hammack, T. Lee, C. Carter, I.B. Matveev, Combustion dynamics of plasma-enhanced premixed and nonpremixed flames, IEEE Trans. Plasma Sci. 38 (2010) 3265–3271.
[146] Luca Massa, Jonathan B. Freund, Plasma-combustion coupling in a dielectric-barrier discharge actuated fuel jet, Combust. Flame 184 (2017) 208–232.
[147] Wenting Sun, Mruthunjaya Uddi, Sang Hee Won, Timothy Ombrello, Campbell Carter, Yiguang Ju, Kinetic effects of non-equilibrium plasma-assisted methane oxidation on diffusion flame extinction limits, Combust. Flame 159 (2012) 221–229.
[148] Rong Feng, Yuhui Huang, Jiajian Zhu, Zhenguo Wang, Mingbo Sun, Hongbo Wang, Zun Cai, Ignition and combustion enhancement in a cavity-based supersonic combustor by a multi-channel gliding arc plasma, Exp. Therm. Fluid Sci. 120 (2021) 110248.
[149] Mahsa Kheirollahivash, Fariborz Rashidi, Mohammad Mahdi Moshrefi, Experimental study and kinetic modeling of methane decomposition in a rotating arc plasma reactor with different cross-sectional areas, Int. J. Hydrog. Energy 44 (2019) 17460–17469.
[150] Chloe E. Dedic, James B. Michael, Thermalization dynamics in a pulsed microwave plasma-enhanced laminar flame, Combust. Flame 227 (2021) 322–334.
[151] Changming Gong, Lin Yi, Kang Wang, Kuo Huang, Fenghua Liu, Numerical modeling of plasma-assisted combustion effects on firing and intermediates in the combustion process of methanol–air mixtures, Energy 192 (2020) 116598.
[152] Changming Gong, Jiawei Yu, Kang Wang, Jiajun Liu, Wei Huang, Xiankai Si, Fuxing Wei, Fenghua Liu, Yongqiang Han, Numerical study of plasma produced ozone assisted combustion in a direct injection spark ignition methanol engine, Energy 153 (2018) 1028–1037.
[153] James A. Miller, Raghu Sivaramakrishnan, Yujie Tao, C. Franklin Goldsmith, Michael P. Burke, Ahren W. Jasper, Nils Hansen, Nicole J. Labbe, Peter Glarborg, Judit Zádor, Combustion chemistry in the twenty-first century: developing theory-informed chemical kinetics models, Prog. Energy Combust. Sci. 83 (2021) 100886.
[154] F. Collin-Bastiani, O. Vermorel, C. Lacour, B. Lecordier, B. Cuenot, DNS of spark ignition using analytically reduced chemistry including plasma kinetics, Proc. Combust. Inst. 37 (2019) 5057–5064.
[155] Xingqian Mao, Aric Rousso, Qi Chen, Yiguang Ju, Numerical modeling of ignition enhancement of $CH_4/O_2/He$ mixtures using a hybrid repetitive nanosecond and DC discharge, Proc. Combust. Inst. 37 (2019) 5545–5552.
[156] Xingqian Mao, Qi Chen, Aric C. Rousso, Timothy Y. Chen, Yiguang Ju, Effects of controlled non-equilibrium excitation on $H_2/O_2/He$ ignition using a hybrid repetitive nanosecond and DC discharge, Combust. Flame 206 (2019) 522–535.
[157] Y. Li, Y. Wu, Research progress and outlook of flow control and combustion control using plasma actuation, Sci. Sin. Technol. 50 (2020) 1252–1273.
[158] J.K. Lefkowitz, Plasma assisted combustion: fundamental studies and engine applications, PhD Dissertation, Princeton University, 2016.
[159] S. Pancheshnyi, B. Eismann, G.J.M. Hagelaar, L.C. Pitchford, available at: http://www.zdplaskin.laplace.univ-tlse.fr, 2008.
[160] Gerjan Hagelaar, available at: http://www.bolsig.laplace.univ-tlse.fr, 2005.

[161] Joseph K. Lefkowitz, Peng Guo, Aric Rousso, Yiguang Ju, Species and temperature measurements of methane oxidation in a nanosecond repetitively pulsed discharge, Philos. Trans. R. Soc. A 373 (2014) 0333.
[162] M. Fast, M. Assadi, S. De, Development and multi-utility of an ANN model for an industrial gas turbine, Appl. Energy 86 (2009) 9–17.
[163] C.M. Bartolini, F. Caresana, G. Comodi, L. Pelagalli, M. Renzi, S. Vagni, Application of artificial neural networks to micro gas turbines, Energy Convers. Manag. 52 (2011) 781–788.
[164] Z. Liu, I.A. Karimi, Gas turbine performance prediction via machine learning, Energy 192 (2020) 116627.
[165] Rashed Kaiser, Songkil Kim, Donggeun Lee, Deep data analysis for aspiration pressure estimation in a high-pressure gas atomization process using an artificial neural network, Chem. Eng. Process. - Process. Intensif. 153 (2020) 107924.
[166] Soteris A. Kalogirou, Artificial intelligence for the modeling and control of combustion processes: a review, Prog. Energy Combust. Sci. 29 (6) (2003) 515–566.
[167] Yan Zhang, Shijie Xu, Shenghui Zhong, Xue-Song Bai, Hu Wang, Mingfa Yao, Large eddy simulation of spray combustion using flamelet generated manifolds combined with artificial neural networks, Energy AI 2 (2020) 100021.
[168] Yeseul Park, Minsung Choi, Kibeom Kim, Xinzhuo Li, Chanho Jung, Sangkyung Na, Gyungmin Choi, Prediction of operating characteristics for industrial gas turbine combustor using an optimized artificial neural network, Energy 213 (2020) 118769.
[169] L. Zhong, Q. Gu, B. Wu, Deep learning for thermal plasma simulation: solving 1-D arc model as an example, Comput. Phys. Commun. 257 (2020) 107496.